Cellular and immunological mechanisms mediate reservoir host specialization by genotypically variable microparasites

Yi-Pin Lin[1,2#]*, Danielle M. Tufts[3#], Alan P. Dupuis, II[1], Matthew Combs[3], Ashley L. Marcinkiewicz[1], Andrew D. Hirsbrunner[1], Alexander J. Diaz[1], Jessica L. Stout[1], Anna M. Blom[4], Klemen Strle[1], April D. Davis[1], Laura D. Kramer[1,2], Maria A. Diuk-Wasser[3]*

[1]Division of Infectious Diseases, Wadsworth Center, New York State Department of Health, Albany, NY, USA, [2]Department of Biomedical Sciences, State University of New York at Albany, NY, USA, [3]Department of Ecology, Evolution, and Environmental Biology, Columbia University, New York, NY USA, [4]Division of Medical Protein Chemistry, Department of Translational Medicine, Lund University, Malmo, Sweden

Short title: Early defense and pathogen adhesiveness confer spirochete host specialization

Key words: Lyme disease, Host specialization, *Borrelia*, Early immune responses, Adhesion

[#]Contributed equally to this work

*correspondence: Yi-Pin Lin, Ph.D.
Division of Infectious Disease,
Wadsworth Center, New York State Department of Health
120 New Scotland Ave., Albany, NY 12047
Telephone: 518-402-2233; Fax: 518-473-1326
Email: Yi-Pin.Lin@health.ny.gov

*correspondence: Maria A. Diuk-Wasser, Ph.D.
Department of Ecology, Evolution, and Environmental Biology,
Columbia University
1200 Amsterdam Ave., New York, NY 10027
Telephone: 212-854-3355
Email: mad2256@columbia.edu

ABSTRACT (289 words)

Host specialization is an ecological and evolutionary process by which a pathogen becomes differentially adapted to a subset of hosts, restricting its host range. For parasites transmitted by generalist vectors, host specialization is not expected to evolve because of the high cost to lose infections in hosts. Adaptation strategies mediating the process of host specialization thus occur. The causative agent of Lyme disease is multiple species of bacteria, *Borrelia burgdorferi* sensu lato species complex (*Bb*sl), and these bacteria are suited to study host specialization as birds and rodents appear to carry different species of these bacteria. Debate exists about whether there is a host specialization among the strains within a particular species of *Bb*sl, such as *B. burgdorferi* sensu stricto (*Bb*ss). Current evidence supports some *Bb* strains widespread in white-footed mice but others in non-rodent vertebrates, such as birds. To recapitulate that in the laboratory and define the mechanisms for host specialization, we introduced different genotypes of *Bb*ss via tick transmission to American robins and white-footed mice, the Lyme disease reservoirs in North America. Among these strains, we found distinct levels of spirochete presence in the bloodstream and tissues and maintenance by these animals in a host-dependent fashion. We showed that the late stage persistence of these strains largely corresponds to bacterial survival at early infection onsets. We also demonstrated that those early survival phenotypes correspond to spirochete adhesiveness, evasion of complement-mediated killing in sera, and/or not triggering high levels of pro-inflammatory cytokines and antibodies. Our findings thus link host competence to *Bb*ss with spirochete genotypic variation of adhesiveness and inducing/escaping host immune responses, illuminating the potential mechanisms that dictate host specialization. Such information will provide a foundation for further investigation into multi-disciplinary processes driving host specialization of microparasites.

AUTHOR SUMMARY (200 words)

Host specialization arises when microparasites adapt to a subset of available hosts, restricting the host ranges they can infect. The molecular basis and selective pressures for the evolution of host specialization remain unclear. The causative agent of Lyme disease (LD), the bacteria species complex of *Borrelia burgdorferi* sensu lato, is adapted to different vertebrates. However, whether such a differential host adaption also applies to each genotype within the same species is under debate. Further, the mechanisms that drive such host specialization are unclear. We thus introduced three genotypes of one LD bacteria species (*B. burgdorferi* sensu stricto) individually via tick bite to American robins and white-footed mice, the most common LD reservoirs in North America. We found that these genotypes differed in the persistent maintenance by those reservoirs and occurred in a host-specific fashion. The ability of those bacteria for long-term maintenance is linked with their capability to attach to cells and lack of induction of high levels of immune responses at early infection onsets. This work demonstrates the potential mechanisms that dictate host specialization of LD bacteria circulating in natural populations. Such information will pave the road to define the molecular, ecological and evolutionary determinants that drive host-microparasite interactions.

INTRODUCTION

The range of hosts a parasite can infect is arguably one of the most important properties of a parasite because it can determine, among other things, whether a parasite can survive the extinction of a host species and whether it can become established and spread following its introduction to a new area (1, 2). For vector-borne microparasites, host-specialization (defined as the ecological and evolutionary process by which a pathogen becomes differentially adapted and thus restricts its host range to a subset of potential hosts) is expected to evolve when vectors are specialized to competent hosts, as it would lead to microparasite amplification. However, it is much less obvious how and when host-specialization in a vector-borne microparasite can occur when vectors are host-indiscriminate. Given the significant cost incurred when microparasites are inoculated into incompetent hosts, the evolution of host specialization is only expected to occur when it provides a significant selective advantage for the microparasite to overcome cellular or immunological barriers to infection.

The spirochetes of the *B. burgdorferi* sensu lato (s.l.) species complex, the agents of Lyme disease, represent an ideal system to investigate the tradeoffs involved in the evolution of host specialization. *B. burgdorferi* s.l. is maintained in an enzootic cycle between generalist ticks of the *Ixodes ricinus* complex and reservoir hosts, including small and medium-sized mammals, birds, and reptiles (3-5). Despite being transmitted by the same generalist vector, some *Borrelia burgdorferi* s.l. genospecies in Europe are almost exclusively associated with a host taxa (e.g. *B. afzelii* in rodents; *B. garinii* in avian hosts). In contrast, *B. burgdorferi* sensu stricto (hereafter *B. burgdorferi*) in North America is considered a host generalist as it has been isolated from multiple classes of vertebrate animals including mammalian and avian hosts (3, 6-8). However, laboratory infection studies indicate that *B. burgdorferi* fitness varies in different hosts (9, 10). In natural

97 populations, weak associations have been found between hosts and particular *B. burgdorferi*
98 genotypes defined by polymorphic markers, such as *ospC* or 16S-23S rRNA intergenic spacer type
99 (RST) (11-13). An intriguing possibility is that the partially and regionally constrained host
100 associations observed in *B. burgdorferi* genotypes represent an incipient evolutionary process of
101 host specialization (4, 12, 14-17). That is, *B. burgdorferi* may be on an evolutionary path to
102 diversify into host specialized genospecies, similar to the *B. burgdorferi* s.l. genospecies in Europe.
103 However, the molecular processes underlying such diversification and the extent to which they
104 would drive genome-wide diversification in *B. burgdorferi* s.l. remain under debate.

105 Multiple-niche polymorphism (MNP), or diversifying selection, has been proposed as a
106 balancing selection mechanism maintaining the diversity of *B. burgdorferi* genotypes through
107 adaptation to host 'niches' (11, 12, 18, 19). This model was applied to the maintenance of the
108 polymorphism in OspC, one of the most diverse Lyme borreliae antigens that is heavily targeted
109 by the vertebrate immune system (20-22). Alternatively (or concurrently), the OspC
110 polymorphism could be maintained in a host-independent manner, through negative frequency-
111 dependent selection, a form of balancing selection driven by adaptive immune response. Thus,
112 bacterial populations carrying rare genotypes have a selective advantage over common genotypes
113 and are thus maintained in the population (14, 17, 23-25). Theoretical studies have examined
114 patterns of OspC diversity predicted by proposed eco-evolutionary mechanisms in different
115 ecological settings (25-28), but a mechanistic understanding of the cellular and immunological
116 mechanisms mediating strain-host interactions is critical to disentangle these multiple co-occurring
117 selective pressures.

118 In this study, we simultaneously assessed cellular and immunological mechanisms that mediate
119 strain-host interactions using three strains to represent variable *ospC* genotypes of *B. burgdorferi*

120 and North American rodent and avian reservoir hosts, American robins (hereafter robins) and
121 white-footed mice (*Peromyscus leucopus*), respectively. We aimed to determine which cellular
122 and immunological mechanisms mediate variation in strain-host fitness, measured as the efficiency
123 of *B. burgdorferi* transmission to feeding larval ticks. Specifically, we identified genotypic
124 differences across *B. burgdorferi* interacting with hosts in (1) the role of complement inhibition
125 and inflammation induction; (2) the role of bacterial adhesion; (3) the role of antibodies in driving
126 late stage persistence in specific hosts and (4) transmission efficiency to larval ticks. By
127 characterizing these mechanisms, we aimed to identify plausible selective pressures that shape the
128 composition of *B. burgdorferi* strain community, its diversity and population dynamics.
129

130 **RESULTS**

131 ***B. burgdorferi* B31-5A4, 297, and cN40 differed in their adhesiveness to fibroblasts, *ex vivo***
132 **cytokine induction, and infection establishment in robins and *Peromyscus* mice.** To study the
133 genotypic variation for *B. burgdorferi* and its capability to initiate infection in reservoir hosts, the
134 cloned *B. burgdorferi* strains B31-5A4, 297, and cN40 belonging to different genotypes and
135 displaying similar growth rates *in vitro* were used in this study (Table S1 and Fig. S1). Bacterial
136 burdens at inoculation sites of skin and in blood were determined at 1 day after each of these strains
137 was intradermally introduced into robins and white-footed mice. We did not detect any of these
138 strains in robin blood (Fig. S2A), in agreement with no hematogenous dissemination at such an
139 early time point (29). However, we found that B31-5A4 and cN40 showed higher spirochete
140 burdens at the initial injection sites, compared to mock-infected robins (Fig 1). The injection sites
141 from only two out of four 297-inoculated robins had spirochete burdens higher than detection
142 limits (10 bacteria per 100ng of DNA from tissues), leading to non-significant differences in the

143 levels of colonization from mock-infected robins (Fig. 1A). Similarly, we did not observe
144 spirochete burdens higher than detection limits of any of these strains in the blood of white-footed
145 mice (Fig. S2B). We observed the levels of B31-5A4 and 297 higher than detection limit at the
146 inoculation site (~10^2 bacteria per 100ng of DNA); only two of five white-footed mice produced
147 cN40 bacterial loads greater than the detectable threshold limit, resulting in non-significant
148 differences in burdens from mock-infected mice (Fig. 1B). These findings indicate B31-5A4, 297,
149 and cN40 have the capacity to establish infection selectively in robins and white-footed mice.

150 As the burdens of *B. burgdorferi* during infection initiation can be attributed to differences in
151 spirochete attachment to cells or clearance by host inflammatory responses, we incubated B31-
152 5A4, 297, and cN40 with fibroblasts isolated from robin or white-footed mouse for 1h and
153 determined the levels of bacterial attachment using fluorescent microscopy (Fig. S3). A non-
154 adhesive *B. burgdorferi* strain B314 was also included as control (Table S1). We found that B31-
155 5A4, 297, and cN40 bind to robin fibroblasts at greater levels compared to B314 (Fig. 1C and D).
156 Whereas B31-5A4 and cN40 bound to robin fibroblasts more than 2.9-fold higher levels than 297
157 (Fig. 1C), B31-5A4 and 297 attached to white-footed mouse fibroblasts at least 1.6-fold higher
158 levels than cN40 (Fig. 1D). To determine whether B31-5A4, 297, and cN40 trigger differential
159 pro-inflammatory responses in fibroblasts from different reservoir origins, we measured the
160 expression levels of the genes encoding pro-inflammatory cytokines, IFNγ and TNF, or the
161 proteins related to these cytokines after incubating cells with each of the spirochete strains for 24h.
162 The expression levels of housekeeping genes (18S rRNA and β-actin) were also included as
163 controls. We did not detect significantly higher levels of expression for each of the genes in any
164 spirochete-treated cells, compared to mock-treated cells, until the spirochete to cell ratio reached
165 1:100 (Fig. 1E to J and S4). At spirochete to cell ratio at 1:100, the B31-5A4- or cN40-treated

166 robin fibroblasts expressed similar levels of tested cytokines to the cells under mock treatment
167 while 297-incubated cells had 4.2- and 5.8-fold greater expression of IFNγ and TNF-induced
168 protein than mock-treated cells, respectively (Fig. 1F and G). Conversely, while white-footed
169 mouse fibroblasts incubated with B31-5A4 or 297 expressed those cytokines indistinguishably
170 from mock-treated cells, cN40-treated cells showed a 4.6- and 30.1-fold higher expression of IFNγ
171 and TNF, respectively, than the cells under mock treatment (Fig. 1I and J). These results suggest
172 that *B. burgdorferi* B31-5A4, 297, and cN40 differ in their fibroblast adhesiveness and cytokine
173 induction in a host-dependent fashion.
174
175 **Ticks acquired different levels of *B. burgdorferi* B31-5A4, 297, and cN40 from robins and**
176 **white-footed mice infected with each of these spirochetes strains.** To compare the reservoir
177 host competence to B31-5A4, 297, and cN40, we assessed spirochete transmission from host to
178 feeding larvae. Unfed *I. scapularis* nymphs were allowed to feed on robins or white-footed mice
179 until repletion (Fig. 2A). We subsequently measured bacterial loads in fed nymphs and found
180 indistinguishable burdens between these ticks (~10^4 bacteria per nymph), indicating no differences
181 of the ability for any tested strain to survive in fed nymphs (Fig. S5).
182 We then placed *I. scapularis* larvae on robins or white-footed mice at different time points to
183 determine spirochete burdens and the percent positivity of spirochete-positive larvae (Fig. 2A).
184 The spirochete burdens in uninfected (control) robin-derived larvae were below the detection limit
185 of the burdens (10 bacteria per tick), resulting in zero spirochete positivity at 14, 28, 35, and 56
186 days post nymph feeding (dpf) (Fig. 2B to F and Table 1). At least 18% of larvae feeding on B31-
187 5A4-, 297-, or cN40-infected robins were spirochete positive at all time points with greater than
188 detection limits of bacterial loads, indicating robins' ability to persistently maintain and transmit

189 these strains (Fig. 2C to F and Table 1). The percent positivity of fed larvae carrying cN40 were
190 at least 1.7-fold greater than those harboring 297 at all four time points and more than 1.5-fold
191 higher than those carrying B31-5A4 at 28, 35, and 56 dpf ($p < 0.05$, Fig. 2B and Table 1). Moreover,
192 the cN40-infected larvae had greater than 4.8-fold higher bacterial loads than the 297-infected
193 larvae at all time points and more than 6.8-fold greater than those in B31-5A4-infected larvae at
194 28, 35, and 56dpf (Fig. 2C to F). These data suggest that the cN40 is maintained and transmitted
195 more efficiently in robins than B31-5A4 and 297.

196 Similarly, we found bacterial burdens lower than detection limits in the larvae feeding on
197 uninfected (control) mice, resulting in zero spirochete positivity (Fig. 2G to K, Table 1). At least
198 9% of the larvae feeding on B31-5A4-, 297-, or cN40-infected mice were positive throughout the
199 experiment (Fig. 2G and Table 1) with bacterial loads higher than detection limits (Fig. 2H to K),
200 except that larvae infected with cN40 had similar spirochete burdens to uninfected mouse-derived
201 larvae at 56dpi. These data indicate the ability of white-footed mice to maintain and transmit these
202 strains. We found 1.3 and 1.2-fold lower spirochete positivity in larvae infected with 297,
203 compared to that in larvae infected with B31-5A4 at 28 and 35 dpf, respectively ($p< 0.05$, Fig. 2G
204 and Table 1 (Fig. 2I and J). Finally, the larvae infected with cN40 showed more than 2.9-fold lower
205 spirochete positivity ($p < 0.05$, Fig. 2G and Table 1) and had at least 69-fold less bacterial burdens
206 than B31-5A4- and 297-infected ticks throughout the experiments (Fig. 2H to K). These data
207 suggest less capability of white-footed mice to maintain and transmit cN40 than B31-5A4 or 297.
208

209 ***B. burgdorferi* B31-5A4, 297, and cN40 varied in their capability to trigger bacteremia and**
210 **persistently colonize robins and white-footed mice.** We next determined the ability of B31-5A4,
211 297, and cN40 to survive in the bloodstream of robins and white-footed mice (Fig. 2A). We found

212 that robins infected with cN40 develop greater levels of bacteremia at 7, 14, and 21dpf than the
213 uninfected robins, which had undetectable levels of spirochete burdens (10 bacteria per 100ng
214 DNA, Fig. 3A to C). However, this strain was under detection limits at 28dpf, consistent with early
215 transient bacteremia triggered by Lyme borreliae (Fig. 3D) (30). The robins infected with 297 had
216 spirochete burdens not detected until 14dpf that then dwindled to undetectable levels at 21dpf (Fig.
217 3A to C). Though B31-5A4 was capable of inducing bacteremia in robins at 7 and 14dpf, this strain
218 did not stay detectable at 21dpf (Fig. 3A to C). These results indicate the ability of cN40 to induce
219 long-lasting bacteremia in robins, compared to other strains, and 297 displayed delayed onsets of
220 bacteremia. Like uninfected robins, uninfected white-footed mice did not have bacteremia at the
221 levels above the detection limit throughout the experiment, and no spirochetes were detected in
222 any *B. burgdorferi*-infected mouse blood at 21 and 28dpf (Fig. 3E and H). B31-5A4 and 297 were
223 detectable in the mouse blood at 7 and 14 dpf (3 and 4 out of 5 mice) at higher levels of bacteremia
224 than uninfected mice ($p < 0.05$, Fig. 3E and F). However, the majority of mice infected with cN40
225 did not have detectable bacteremia (3/5 and 5/5 mouse blood had burdens below detection limits
226 at 7 and 14dpf, respectively) (Fig. 3E and F). These data suggest that cN40 is less capable of
227 surviving in the white-footed mouse bloodstream than B31-5A4 and 297, in contrast to results
228 derived from robins.

229 We also evaluated the ability of B31-5A4, 297, and cN40 to colonize robins and white-footed
230 mice tissues and be detectable after animals were sacrificed at 64dpf (Fig. 2A). Robins infected
231 with each of these strains had greater spirochete burdens in skin than uninfected robins, bacterial
232 loads of which were undetectable ($p < 0.05$, Fig. 3I). In addition, spirochetes were detected at
233 greater burdens in the heart and brain of cN40-infected robins and the heart of robins infected with
234 B31-5A4, compared to respective tissues from uninfected robins ($p < 0.05$, Fig. 3J and K).

235 However, the average burdens of B31-5A4, 297 or cN40 in the livers from spirochete-infected
236 robins were below detection limits (Fig. 3L). These data showed persistent skin colonization of
237 strains B31-5A4, 297, and cN40 in robin, but the ability of each strain to colonize other tissues
238 varied (Fig. 3I to L). We also measured the bacterial burdens at 64dpf in the tissues from white-
239 footed mice infected with each of these strains. We detected spirochetes in ears, tibiofemoral joints,
240 heart and bladder from mice infected with B31-5A4 or 297 (~10^2 to 10^3 bacteria per 100ng of
241 DNA from tissues). Such burdens were greater than those in uninfected mice throughout the
242 experiment (Fig. 3M to P). However, the spirochete loads in cN40-infected mouse tissues were
243 undetectable (Fig. 3M to P). These findings demonstrated the ability of B31-5A4 and 297 but not
244 cN40 to persistently colonize white-footed mice.
245
246 **Robin but not white-footed mouse complement differentiated the ability of *B. burgdorferi***
247 **B31-5A4, 297, and cN40 to survive in sera.** To define the capability of B31-5A4, 297, and cN40
248 to evade complement-mediated killing, we evaluated the percent survival after incubation of these
249 strains individually with the sera from uninfected robins or white-footed mice by counting the
250 number of motile bacteria under microscopes. More than 95% of all tested strains including a
251 serum sensitive control strain, *B. burgdorferi* B313 (31), survived in heat inactivated robin sera,
252 in which the heat sensitive components such as complement were not functional (Fig. 4A and
253 Table S1). Less than 16% of B313 remained motile, verifying the bactericidal activity of these
254 robin sera (Fig. 4A). More than 85% of B31-5A4 and cN40 were alive, but only 50% of 297 was
255 motile after incubated with robin sera (Fig. 4A). However, all strains survived at similar levels
256 (greater than 80% of live spirochetes) in the sera pre-treated with OmCI, which inactivates robin
257 complement by abolishing the lytic activity towards gram negative bacteria (Fig. 4B) (32). These

258 results indicate that the 297 is more vulnerable to robin complement-mediated killing than B31-
259 5A4 and cN40. We also determined the ability of spirochete strains to evade killing by white-
260 footed mouse complement in the similar fashion. Greater than 95% of B313, B31-5A4, 297, and
261 cN40 survived in heat inactivated *Peromyscus* mouse sera (Fig. 4C). Whereas only 29% of B313
262 remained motile after treated with these sera, more than 97% of other tested strains were alive in
263 the sera (Fig. 4C). More than 93% of tested strains remained motile in white-footed mouse sera
264 pre-treated with CVF, which inactivates mammal complement (Fig. 4D) (33). These results
265 indicate that all tested strains evade the killing by white-footed mouse complement at
266 indistinguishable levels.
267
268 **Robins and white-footed mice generated different levels of pro-inflammatory cytokines in**
269 **response to early infection of *B. burgdorferi* B31-5A4, 297, and cN40.** We compared the levels
270 of pro-inflammatory cytokines, IFNγ and TNFα, in the sera derived from robin- and white-footed
271 mice at different times during the infection. We found similar levels of IFNγ and TNFα in robins
272 prior to the infection among different infection groups ($p > 0.05$, Fig. 5A and E). At 7dpf, though
273 robins infected with B31-5A4 or cN40 displayed no significantly different levels of those
274 cytokines from uninfected robins, robins infected with 297 produced 2.5 to 4-fold greater levels
275 of IFNγ and TNFα than those uninfected birds, respectively (Fig. 5B and F). These levels
276 diminished to baseline at 14dpf. In contrast to robins at 7dpf, mice infected with cN40 displayed
277 3.2- to 11.4-fold higher levels of these cytokines than uninfected mice at this time point,
278 respectively, while mice infected with 297 had no different levels of those cytokines, compared to
279 uninfected mice (Fig. 5J and N). Note that mice infected with B31-5A4 had slightly greater levels
280 of IFNγ ($p < 0.05$, Fig. 5J) but no significantly different levels of TNFα at 7dpf ($p > 0.05$, Fig. 5N),

compared to uninfected mice. These data indicate differences of pro-inflammatory cytokine induction by each of these spirochete strains, particularly at early stages of robin and white-footed mouse infection.

Robins and white-footed mice developed distinct levels of bactericidal antibodies during early infection of *B. burgdorferi* B31-5A4, 297, or cN40. We aimed to quantitatively measure the levels of antibodies induced by the infection of B31-5A4, 297, and cN40. To avoid the confounding factors of strain-specific antibody recognition observed previously (10, 34), we mixed these strains and determined the IgG titers against such mixtures in robins infected with B31-5A4, 297, or cN40. We found that the robins infected with either strain develop higher anti-spirochete IgG titers than uninfected robins at 14, 21, and 28dpf (Fig. 6C to E). cN40 triggered greater levels of such IgGs than other strains at 21 and 28 dpf whereas 297 induced IgG titers higher than those titers triggered by other strains at 7dpf (Fig. 6B, D and E). Further, we found that white-footed mice infected with each of these strains have anti-spirochete IgG titers at more robust levels than uninfected mice at 14, 21, and 28dpf (Fig. 6G to J). cN40 induced lower titers of such IgG at 21 and 28dpf but higher titers at 7dpf, compared B31-5A4 and 297 (Fig. 6G, I and J). These results indicate that B31-5A4, 297, and cN40 differ in their ability to induce antibodies, and such differences depend on the hosts and infection onset.

The levels of antibodies against B31-5A4, 297, or cN40 at 7dpf in robins and *Peromyscus* mice negatively corresponded to the ability of these hosts to carry spirochetes (Fig. 2B and G). This finding raised a hypothesis that such correspondences are mediated by bactericidal activities of those antibodies. We thus tested this hypothesis by incubating the mixture of B31-5A4, 297, and cN40 with different dilution rates of sera from robins or white-footed mice infected with each of

304 these strains at 7dpf. We found that B31-5A4- and cN40-derived robin sera did not kill spirochetes
305 at any of the tested dilution rates, similar to sera from uninfected robins. However, 297-derived
306 sera eliminated 50% of spirochetes at the dilution rate of 1:52× (Fig. 6K). Conversely, B31-5A4-
307 and 297-derived white-footed mouse sera did not eliminate spirochetes, similar to the sera from
308 uninfected mice. However, cN40-derived sera eliminated 50% of spirochetes at the dilution rate
309 of 1:32× (Fig. 6L). These finding showed different levels of bactericidal activities from the
310 antibodies produced by B31-5A4-, 297-, or cN40-infected robins and white-footed mice early
311 during infection.
312

313 **DISCUSSION**

314 Theory predicts that generalist vectors should select for generalist pathogens, to minimize their
315 loss to incompetent hosts. Host-specialized genospecies in *B. burgdorferi* s.l. thus represent a
316 paradox, with the intriguing possibility of incipient host specialization within genotypes of the
317 generalist *B. burgdorferi*. We present evidence of molecular mechanisms that differentially
318 influence the ability of three strains of *B. burgdorferi* to colonize, disseminate to distal tissues,
319 evade host immune responses, and transmit from the host to feeding ticks between two
320 representative natural hosts (Fig. 7). We found that cellular and immunological mechanisms act
321 mostly synergistically, resulting in increased fitness of strain cN40 in robins and 297 in white-
322 footed mice. Contrary to theoretical expectations, strain B31-5A4 was able to efficiently infect
323 both hosts, with higher fitness than the 'white footed mouse-specialized' strain, 297, and
324 intermediate fitness in robins. The synergistic nature of those cellular and immunological
325 mechanisms indicates a strong selective pressure for the evolution of host specialization, as
326 predicted by the MNP theory. However, the highest overall fitness of B31-5A4 does not support

327 the existence of tradeoffs, with this strain having very high fitness in both representative hosts.
328 This higher fitness advantage is consistent with the greater overall prevalence for the genotype of
329 this strain (RST type 1/OspC type A) circulated in Lyme disease prevalent regions of North
330 America (10, 13, 35-38).

331 Multiple mechanisms were tested in this study for their role in contributing to host specialization
332 of *B. burgdorferi*. At one day after intradermal infection of spirochetes, we found that *B.*
333 *burgdorferi* B31-5A4 and cN40 colonized robin inoculation sites (skin tissue) more efficiently
334 than 297, whereas B31-5A4 and 297 colonized the inoculation sites of white-footed mice at higher
335 levels than cN40. We also found that these strains differed in their capability to attach to robin and
336 white-footed mouse skin fibroblasts *in vitro*. These results showed that strain-to-strain variability
337 of fibroblast adhesion is host-dependent and corresponds to the ability of *B. burgdorferi*
338 spirochetes to colonize the inoculation sites of these hosts immediately after infection. This
339 supports prior findings of Lyme borreliae strains varying in their adhesive activities (39),
340 demonstrating the role of such cellular processes (adhesion) in conferring strain-host associations.

341 However, the levels of robin fibroblast adhesion of B31-5A4, 297, and cN40 did not perfectly
342 agree to strain colonization of other tissues (e.g. brain and liver) in robins at 64 days after fed on
343 by *B. burgdorferi*-infected nymphs. Additionally, strain 297 colonized robin skin at similar levels
344 to B31 or cN40 at 64 dpf, but this strain attached to robin fibroblast at lower levels than other
345 strains. These disagreements between fibroblast adhesion/early colonization of inoculation sites
346 and tissue colonization at later stages suggest the possibility of adhesion-independent mechanisms
347 to determine strain-host associations. In fact, the complement system is the first line of immune
348 defense in vertebrate animal sera and confers Lyme borreliae clearance as soon as infection begins
349 (40, 41). Our findings of greater percentages of B31-5A4 and cN40 surviving in robin sera,

350 compared to those of 297, mirror the trends of these spirochete strains maintained at earlier
351 infection onsets (e.g. 14 dpf) and early bloodstream survival of *B. burgdorferi* (e.g. 7 dpf). These
352 results imply that the host complement plays a role in determining spirochete genotype-specific
353 robin competence. In contrast, all three *B. burgdorferi* strains showed similar levels of survival in
354 the presence of white-footed mouse sera, suggesting a non-complement defense mechanism to
355 dominate the association of white footed mice with these spirochetes.

356 In fact, cytokines are generally triggered shortly after pathogen invasions, often leading to
357 activation of different pathways and downstream bactericidal responses as a bottleneck of infection
358 initiation (i.e. recruitment of innate and adaptive immune cells) (42-46). *Borrelia burgdorferi*
359 strain-to-strain variability in inducing pro-inflammatory cytokines has been observed in humans,
360 *M. musculus*, and *P. leucopus* mice or from cells derived from these animals (47-53). In humans,
361 the levels of multiple cytokines are positively correlated with disease severity but are independent
362 from spirochete burdens (47, 48, 54-56). We found that three tested *B. burgdorferi* strains differed
363 in their ability in robins and white-footed mouse fibroblasts to induce the expression of two pro-
364 inflammatory cytokines and their related proteins, IFNγ, TNFα, and TNFα-induced proteins. Such
365 differences also matched the variation of these strains to trigger IFNγ and TNFα during early
366 infection. The ability of these strains to induce those pro-inflammatory cytokines were negatively
367 associated with the larvae percent positivity from the infection of these *B. burgdorferi* strains.
368 These results raised the hypothesis that less robust host cytokine induction by spirochetes
369 facilitates reservoir competence, and differences in cytokine induction by genotypically distinct
370 spirochetes shape Lyme borreliae-reservoir associations.

371 Following the induction of innate immune responses, the adaptive responses including
372 antibodies are essential in Lyme borreliae clearance by vertebrates (42, 57, 58). Distinct levels of

373 antibodies have been observed during the infection by different spirochete strains (10, 59). We
374 observed at 7 dpf that 297 and cN40 trigger higher titers of anti-*B. burgdorferi* IgG in robins and
375 white-footed mice, respectively, compared to other spirochete strains. Furthermore, *B. burgdorferi*
376 was selectively eliminated by the sera collected at 7dpf from robins infected with 297 or white-
377 footed mice infected with cN40, suggesting that the antibody response varies among different
378 spirochete strain-host pairings. Interestingly, a previous study showed variable IgG levels against
379 lp36- and lp28-1-derived proteins in white-footed mice infected with different *B. burgdorferi*
380 strains (10). However, those lp36- and lp28-1-derived proteins were generated from a *B.*
381 *burgdorferi* strain (*B. burgdorferi* strain B31), leading to the possibility that allelic-specific
382 recognition is the result of antigenic sequence variation among spirochete strains (10, 34, 60-62).
383 Thus, that finding does not rule out the possibility of the antibodies against other spirochete
384 proteins to confer *B. burgdorferi* clearance. Our finding of early antibody-mediated bactericidal
385 activities in robin and white-footed mouse sera highlights the potential role of antibodies in
386 dictating pathogen-host associations. We observed high titers of antibody responses at late time
387 points (21 and 28 dpf) in robins infected with cN40 and mice infected with B31-5A4- or 297.
388 Nonetheless, cN40 is persistently maintained in robins whereas B31-5A4 and 297 efficiently
389 survive in long term in white-footed mice. Such observations are consistent with the evidence of
390 pathogen-specific antibodies present in persistently infected animals (63-65). These results thus
391 suggest inefficient spirochete elimination by those antibodies at later stages of infection. That
392 inefficient pathogen killing could be because of the onset-dependent reduction of highly antigenic
393 spirochete proteins (i.e. downregulation of OspC at late infection onsets) (66-70), constantly
394 changing features of antigen sequences to evade antibody responses (i.e. VlsE) (71-73), or the
395 rapid dissemination of spirochetes to the sites less vulnerable to antibody-mediated clearance (74).

396 Our results suggest spirochete adhesiveness and early immune responses as the cellular and
397 immunological mechanisms that differentially confer spirochete fitness in reservoir-strain-host
398 combinations (Fig. 7). Both mechanisms could play in concert to determine *B. burgdorferi* strain-
399 to-strain variation in host fitness. Our findings support previous studies which determined that
400 some polymorphic Lyme borreliae proteins confer these immune response functions in a variant-
401 specific manner, and such manner is host dependent. (30, 31, 60, 63, 64, 75-80). The potential for
402 host specialization caused by genome-wide diversification has been illustrated by the recent
403 definition of a new species of *B. burgdorferi* s.l., *B. bavariensis*, which was previously considered
404 as a genotype of the avian associated species, *B. garinii*. Such a redefinition is based on the
405 variations in chromosomal housekeeping genes and the association of this species with rodents,
406 unlike other *B. garinii* strains (81). This reclassification reflects to how host adaptation can lead to
407 speciation in Lyme borreliae (82). Prior field studies along with our current laboratory evidence
408 showing incipient host specialization raises the possibility of diversification of *B. burgdorferi* in
409 North America into multiple genospecies. Here, we used a controlled laboratory setup to
410 demonstrate distinct differences in fitness of North American Lyme disease reservoir hosts to
411 different *B. burgdorferi* strains. The molecular mechanisms supported by our findings here provide
412 a potential model of how specific adaptations may lead to specialization even with a significant
413 cost in lost propagules to incompetent hosts. The identified mechanisms can illuminate future
414 modeling studies of parasite-host dynamics that can be validated in local populations and increase
415 the understanding of the associations between hosts and microparasites.
416

417 **MATERIALS AND METHODS**

418 **Ethics statement.** All experiments involved in American robins (*Turdus migratorius*) and white-
419 footed mice (*Peromyscus leucopus*) were performed in strict accordance with all provisions of the
420 Animal Welfare Act, the Guide for the Care and Use of Laboratory Animals, and the PHS Policy
421 on Humane Care and Use of Laboratory Animals. Additionally, the protocol was approved by the
422 Institutional Animal Care and Use Committee (IACUC) of Wadsworth Center, New York State
423 Department of Health (Protocol docket number 18-412 and 19-451), and Columbia University
424 (Protocol docket number AC-AAAY2450), and City University in New York Advanced Science
425 Research Center (Protocol number ASRC AUP 2016-20). To mist net robins, personnel were
426 approved on scientific collecting permits (USFWS Collecting Permit MB035731; NYSDEC
427 Permit #1236).
428
429 **Bird, Mouse, Tick, and Bacterial strains.** From June-July, 2019 and July, 2020, American robins
430 were mist netted around the property of Griffin Laboratory of Wadsworth Center, New York State
431 Department of Health at Albany, NY. This site was selected given previously reported low tick
432 abundance, thus minimizing the probability of previous tick exposure. Sera were collected from
433 32 and 17 robins in 2019 and 2020, respectively, using BD Microtainer Capillary Blood Collector
434 tubes (Fisher Scientific, Hampton, NH, USA) to assess previous infection with *B. burgdorferi*
435 infection by the methods previously described (32). To confirm seronegative status, robins were
436 quarantined for two weeks at 25°C on a 12L:12D (light: dark) cycle by housing them in cages with
437 a wire bottom, under which a water moat was placed. If replete ticks were found while the birds
438 were in quarantine, quantitative PCR (qPCR) was used to determine the spirochete burdens in
439 those ticks (see "Quantification of *B. burgdorferi* in infected ticks, tissues, and blood samples" for
440 more details). The birds with spirochete positive ticks attached were removed from the

441 experiments. After two weeks of quarantine, those robins were subjected to additional serological
442 examination as described above, and 40 seronegative juvenile (hatch year) robins were considered
443 non-infectious and used in this study.

444 White-footed mice were purchased from the *Peromyscus* Genetic Stock Center at the University
445 of South Carolina (Columbia, SC). Non-sibling mice were bred in house at Columbia University.
446 Immunodeficient Fox Chase SCID mice (C.B.17 SCID) were obtained from Charles River (Boston,
447 MA) and used to generate infected nymphs for each *B. burgdorferi* strain as described in the
448 "Mouse infection experiments by ticks" section. *Ixodes scapularis* larvae were purchased from the
449 National Tick Research and Education Center, Oklahoma State University (Stillwater, OK). Mice
450 and birds were housed individually and maintained at 21 to 24°C on a 14L:10D (light: dark) cycle
451 and handled humanely. The *B. burgdorferi* strains used in this study were cultivated in BSK-II
452 completed medium as described in Table 1 (83).

453

454 **Determination of spirochete growth curves and generation time.** *Borrelia burgdorferi* strains
455 B31-5A4, 297, and cN40 were cultivated in BSK-II complete media at 33°C in the initial
456 concentration of 5×10^6 ml^{-1}. The concentration of spirochetes was measured prior to incubation
457 and at 24-, 48-, 72-, 96-, 120-, 144-, and 168-h post incubation using a Nikon Eclipse E600 dark
458 field microscope (Nikon, Melville, NY). The generation time of each spirochete strain at the
459 exponential phase was calculated as described previously (84).

460

461 **Robin, C.B.17 SCID mouse, and white-footed mouse infection by intradermal inoculation.**
462 Four to eight week old of male or female white-footed mice, American robins, or C.B.17 SCID
463 mice were intradermally inoculated, using a 27-guage needle, with *B. burgdorferi* B31-5A4, 297,

464 cN40, or BSK-II medium without rabbit sera (1×10^5 bacteria per C.B.17 SCID mouse or 1×10^4
465 bacteria per robin or white-footed mouse) as a control (64). The plasmid profiles and the presence
466 of the shuttle plasmids of each of these *B. burgdorferi* strains were verified prior to infection to
467 ensure no loss of plasmids, as described previously (85-87). The C.B.17 SCID mice were
468 euthanized at 21 days post injection whereas both robins and white-footed mice were sacrificed at
469 one day post injection. The inoculation site of the skin and blood from robins and white-footed
470 mice were collected to quantitatively evaluate spirochete burdens as described in the
471 "Quantification of *B. burgdorferi* in infected ticks, tissues and blood samples" section.
472
473 **Quantification of *B. burgdorferi* in infected ticks, tissues, and blood samples.** The white-footed
474 mouse- or robin-derived replete nymphs were mixed with glass beads and homogenized by a
475 Precellys 24 High-Powered Bead Mill Homogenizer (Bertin, Rockville, MD). DNA was extracted
476 from blood and tissues of white-footed mouse and robin and homogenized ticks using an EZ-10
477 Genomic DNA kit (Biobasic, Amherst, NY). The quantity and quality of DNA for each tissue
478 sample was assessed by measuring the concentration of DNA and the ratio of the UV absorption
479 at 280 to 260 using a nanodrop 1000 UV/Vis spectrophotometer (ThermoFisher Scientific,
480 Waltham, MA). The amount of DNA used in this study was 100 ng for each sample, and the
481 280:260 ratio was between 1.75 to 1.85, indicating the lack of contamination by RNA or proteins.
482 qPCR was performed to quantitate bacterial loads. *Borrelia burgdorferi* genomic equivalents were
483 calculated using an Applied Biosystems 7500 Real-Time PCR system (ThermoFisher Scientific)
484 in conjunction with PowerUp SYBR Green Master Mix (ThermoFisher Scientific), based on
485 amplification of the *B. burgdorferi 16S rRNA* gene using primers 16S rRNAfp and 16S rRNArp
486 (Table S2), as described previously (88). Cycling parameters for SYBR green-based reactions

487 were 50°C for 2 min, 95°C for 10 min, 45 cycles of 95°C for 15 s, and 60°C for 1 min. The number
488 of *16S rRNA* copies was calculated by establishing a threshold cycle (Cq) standard curve of a
489 known number of *16S rRNA* gene copies extracted from *B. burgdorferi* strain B31, and compared
490 to the Cq values of the experimental samples. To assure low signals were not simply a function of
491 the presence of PCR inhibitors in the DNA preparation, we included in all five samples of blood,
492 tibiofemoral joints, and bladders of white-footed mice and the skin, brain, and heart of robins in
493 the B31-5A4 experimental group to amplify β-actin from *P. leucopus* (pActfp and pActrp) and
494 robins (rActfp and rActrp) (Table S2) as an internal standard (64, 89). Note that the primers used
495 to determine the expression of the genes encoding robin actin were based on the mRNA sequences
496 that were translated to protein (Genbank Accession number: PYHW01009720.1) from a closely
497 related avian host, rufous-bellied thrush (*Turdus rufiventris*) due to the lack of sequence
498 information of American robin actin. As predicted, we detected 10^7 copies of the actin gene from
499 100ng of each DNA sample in robins and white-footed mice, ruling out the presence of PCR
500 inhibitors in these samples.
501
502 **Isolation of robin fibroblasts.** The procedures to isolate robin fibroblasts were described
503 previously (90). Five 5mm × 5mm sections of skin were removed from the breast of the euthanized
504 robins, plucked of feathers, washed twice in PBS buffer, and then incubated in the transferring
505 solution until the next step was ready to be performed. The constituents of transferring solution
506 include Dulbecco's modified Eagle medium (DMEM) (Wadsworth media & tissue culture core)
507 with glucose (4.5mg ml^{-1}) (Sigma-Aldrich, St. Louis, MO), sodium pyruvate (110mg l^{-1}) (Sigma-
508 Aldrich), L-glutamine (ThermoFisher Scientific), supplemented with 10% heat-inactivated fetal
509 bovine serum (ThermoFisher Scientific), 2% heat-inactivated chicken serum (Biowest, Riverside,

510 MO, USA), and antibiotics (100U ml^{-1} of mixture of penicillin and streptomycin) (ThermoFisher
511 Scientific). The skin was then submerged in 70% ethanol (Sigma-Aldrich) for 30s, minced using
512 sterile scalpels, and placed in collagenase B at 37ºC overnight (ThermoFisher Scientific). We then
513 applied the mixture of the cells to a 20µm cell strainer and spun down the samples. The pellets
514 containing fibroblasts were re-suspended in growth media and incubated at 37ºC with 5% CO_2.
515 Growth media has the same components as transferring solution except it is supplemented with
516 amphotericin B (ThermoFisher Scientific) to a concentration of 0.25µg/ml. The cells were
517 harvested by trypsinization using Trypsin (0.25% trypsin in DMEM media, ThermoFisher
518 Scientific) and used in the spirochete attachment experiment.
519
520 **Determination of the levels of spirochete attachment to robin and white-footed *mouse***
521 **fibroblasts.** The primary fibroblasts from the neck skin of American robins (see the previous
522 section) and ears of *P. leucopus* acquired commercially (#AG22353, Coriell Institute for Medical
523 Research, Camden, NJ) were cultivated on cover slips in 24-well plates (2×10^5 cells per well).
524 *Borrelia burgdorferi* strains B31-5A4, 297, cN40, or B314 were suspended in BSK-II medium
525 and added to prepared plates (2×10^6 spirochetes per well). The plates were centrifuged at 106g
526 for 5 min and then rocked at room temperature for 1 h. After removing unbound bacteria through
527 washing each well with PBS containing 0.2% BSA, the bound bacteria and cells on the cover slips
528 were fixed using 100% chilled methanol for 1h followed by blocking with PBS containing 0.2%
529 BSA for 1 h. After washing with PBS containing 0.2% BSA, the cover slips were incubated with
530 a fluorescein isothiocyanate (FITC)-conjugated goat anti-*B. burgdorferi* polyclonal antibody
531 (Abcam, Cambridge, MA) for 1h and mounted using ProLong Gold antifade mountant with DAPI
532 fluorescent stain (ThermoFisher Scientific). The spirochetes (green) and the DNA from

533 spirochetes and the nuclei of fibroblasts (blue) were then visualized under overlaid FITC and DAPI
534 filters using an Olympus BX51 fluorescence microscope (Olympus Corporation, Waltham, MA)
535 (Fig. S3). The number of spirochetes from three fields of view were counted in four independent
536 events. The results were presented as the average number of spirochetes per 50 fibroblast cells.
537
538 **Determination of the relative expression levels of the genes encoding IFNγ and TNF or TNF-**
539 **induced proteins in fibroblasts by qRT-PCR.** The procedures for the examination of expression
540 levels in the genes encoding cytokines of fibroblasts were described previously (53). In brief, the
541 primary fibroblasts from robins and white-footed mice were cultivated in 24-well plates (2×10^5
542 cell per well). When the cells were greater than 80% confluent, *B. burgdorferi* strains B31-5A4,
543 297, or cN40 suspended in BSK-II medium were added to corresponding wells on each plate ($2 \times$
544 10^6 and 2×10^7 spirochetes per well for the cell to spirochete ratio (MOI) of 1:10 and 1:100,
545 respectively) for 24h. The cells incubated with BSK-II medium without bacteria (mock-treated
546 cells) were included as a control.
547 After incubation, the supernatant was removed, and the cells were washed with PBS buffer.
548 These fibroblasts were then suspended in Trizol (ThermoFisher Scientific) at room temperature
549 for 1h to inactivate RNase. The procedure of RNA extraction was performed using Direct-Zol
550 RNA MiniPrep Plus Kit (Zymo Research, Irvine, CA) as previously described (84), and DNA was
551 removed using RQ1 RNase-Free DNase (Promega, Madison, WI). We then synthesized cDNA
552 using these RNA samples (1 μg per sample) by qScript cDNA SuperMix (Quanta Bioscience,
553 Beverly, MA). The expression levels of the house keeping genes encoding the 18S rRNA gene
554 from robins (Genbank Accession number: M59402.1) or white-footed mice (Genbank Accession
555 number: AY591913.1) were included as controls. The primers used to quantitate the expression of

556 the genes encoding white-footed mouse IFNγ, TNF, and 18S rRNA, and robin IFNγ, TNFα-
557 induced proteins, and 18S rRNA are listed in Table S2 (89). Note because of the lack of the
558 sequence information of robin cytokines, the primers to determine the expression of these
559 cytokines are based on the mRNA sequences of IFNγ (Genbank Accession number:
560 PYHW01010552.1) and TNFα-induced proteins (Genbank Accession number: PYHW01009717.1)
561 from Rufous-bellied thrush (*Turdus rufiventris*). The quantity and quality of cDNA for each
562 sample was evaluated by obtaining the concentration of DNA and the ratio of the UV absorption
563 at 260 and 280 using a Nanodrop 1000 UV/Vis spectrophotometer (ThermoFisher, Waltham, MA).
564 The resulting ratio between 1.75 and 1.85, indicated the lack of RNA or protein contamination.
565 Samples were applied to an Applied Biosystems 7500 Real-Time PCR System (ThermoFisher) in
566 conjunction with PowerUp SYBR Green Master Mix (ThermoFisher) to detect the expression
567 levels of the above-mentioned genes. The cycling parameters were 50°C for 2 min, 95°C for 10
568 min, and 45 cycles of 95°C for 15 s, and 49°C for 1 min, and the resulting values of threshold
569 cycles (Cq) were determined from duplicate experiments in three independent events. The relative
570 expression of the genes encoding IFNγ, TNF, TNF-induced proteins, or 18S rRNA was presented
571 by normalizing the Cq-derived from each of these cytokines to that of β-actin from respective
572 animals through the following equation (Equation 1).

573 $$\textit{cytokine expression relative to actin} = 2^{-(Cq(cytokines)-Cq(actin))} \quad \text{(Equation 1)}$$

574

575 **Generation of *B. burgdorferi*-infected nymphal ticks.** Four-week-old male and female C.B.17
576 SCID mice were injected with a concentration of $1x10^5$ of either *B. burgdorferi* strain B31-5A4,
577 297, or cN40 via subcutaneous injection. The plasmid profiles and the presence of the shuttle
578 vector of each of these *B. burgdorferi* strains were verified prior to injection to ensure no loss of

579 plasmids, as previously described (85-87). The SCID mice inoculated with BSK-II media without
580 rabbit sera were used to generate uninfected nymphs. A 3 sq. mm. of ear biopsy was collected 7
581 days post injection from each mouse inoculated with a *B. burgdorferi* strain and DNA was
582 extracted using a DNeasy Blood and Tissue kit (Qiagen, Germantown, MD). DNA from ear tissue
583 was subjected to qPCR analysis to verify infection in each host (31). At 14 days post injection,
584 approximately 200 larvae were placed in the ears of anesthetized mice using a paint brush. Mice
585 were anesthetized with isoflurane for 45 min to allow larvae to attach before being housed
586 individually in water bath cages, and the larvae were allowed to feed to repletion, as described
587 previously (31, 91). Engorged larvae were collected, cleaned with 10% bleach and 70% ethanol
588 solutions, and stored in an incubator at 21°C, 95% relative humidity, and a 14L:10D light: dark
589 cycle. Larvae molted into the nymphal life stage in approximately 4-6 weeks and were used in the
590 subsequent experiments with *P. leucopus* mice and robins.
591
592 **Robin and white-footed mouse infection by nymphs.** The timeline of experimental procedures
593 is provided in Fig. 2. Basically, the unfed nymphs carrying B31-5A4, 297, cN40 or unfed,
594 uninfected nymphs were placed in the ear canals of each mouse. Mice were maintained under
595 anesthesia for 60 min to allow nymphs to attach before being placed individually in water bath
596 cages. Approximately 100 to 150 xenodiagnostic larvae were placed on each mouse at 14, 28, 35,
597 and 56 days post nymph feeding using the aforementioned procedure. To permit flat nymphs to
598 feed on robins, robins were placed into a PVC pipe (~2.5-3.0 inches in diameter; 10 inches in
599 length) as described (92). After the unfed nymphs carrying B31-5A4, 297, cN40 or unfed,
600 uninfected nymphs were placed on these robins (10 nymphs per bird), the PVC pipes were covered
601 by a fine mosquito net ('no-see-um' netting, Skeeta, Bradenton, FL) that was secured with a rubber

602 band and then moved into the cages with wired bottom, under which the moat is located. These
603 tick-infested robins were kept in a dark room for 1h to minimize grooming and allow ticks to attach
604 before they were released and returned to the cages. To allow xenodiagnostic larvae feed on robins,
605 approximately 100 to 200 naïve larvae were placed on robins restrained in the PVC pipes as
606 described above at 14, 28, 35, and 56 days post nymph feeding.

607 Blood samples were collected from each animal (robins and *P. leucopus* mice) prior to nymph
608 feeding and at 7, 14, 21, and 28 days post nymph feeding. The skin, heart, liver, and brain from
609 robins and the ears, tibiofemoral joints, heart, and bladder from *P. leucopus* mice were obtained at
610 64 days post nymphs feeding. The blood, tissues and replete nymphs derived from each animal
611 were applied to qPCR to determine spirochete burdens as described in the section "Quantification
612 of *B. burgdorferi* in infected ticks, tissues, and blood samples".

613

614 **Serum resistance assays.** Serum resistance of *B. burgdorferi* strains was determined as described
615 previously with modifications (31, 84). The mid-log phase of *B. burgdorferi* strains B31-5A4, 297,
616 and cN40 as well as a high passage, serum sensitive strain B313 (negative control) were cultivated
617 in triplicate. The resulting spirochete culture was diluted to a final concentration of 5×10^6 bacteria
618 per milliliter into BSK-II medium without rabbit sera. The cell suspensions were mixed with sera
619 collected from naïve white-footed mice or robins (60% spirochetes and 40% sera) in the presence
620 or absence of 2μM of cobra venom factor (CVF) or recombinant *Ornithordorus moubata*
621 complement inhibitor (OmCI). The generation of recombinant OmCI has been described
622 previously (32). The sera incubated at 65ºC for 2-h (heat-inactivated sera) were included as a
623 control. At 0- and 4-h following incubation with sera, the number of motile spirochetes was
624 measured under dark field microscopy. The percent survival of *B. burgdorferi* was calculated by

625 the normalization of motile spirochetes at 4-h post incubation to that immediately after incubation
626 with sera.
627
628 **Determination of the relative levels of IFNγ and TNFα in sera by ELISA.** Due to the lack of
629 commercially available ELISA kits to detect robin cytokines, the kits for chicken IFNγ
630 (ThermoFisher) and TNFα (Genorise, Glen Mills, PA) were used to measure the levels of those
631 cytokines in robins based on the absorption values derived from ELISA. Similarly, the ELISA kits
632 to determine the levels of IFNγ and TNFα from house mouse (*Mus muscuslus*) (Tonbo Bioscience,
633 San Diego, CA) were utilized to detect those cytokines in white-footed mice. We observed the
634 antibodies in the ELISA kits cross reacted with IFNγ and TNFα from robins and white-footed mice.
635 However, the recombinant proteins provided in these kits to generate standard curves were based
636 on the sequences from chicken and house mouse IFNγ and TNFα, potentially leading to the
637 inaccuracy of quantification for those cytokines by normalizing the results obtained from robin
638 and white-footed mouse samples to standard curves. Therefore, we chose to present reservoir
639 animal cytokines as relative levels (arbitrary unit; A.U.), similar to the previous study (93). In brief,
640 the monoclonal capture antibodies that recognized chicken or house mouse IFNγ or TNFα were
641 coated on microtiter plate wells. After blocked by 5% PBS-BSA, the different dilution (1:100×,
642 1:300×, or 1:900×) of sera from robins and white-footed mice at 0, 7, 14, or 21 days post nymph
643 feeding were added to the wells. Wells were washed using PBST buffer (PBS with 0.5% of Tween
644 20) and the detection of antibodies against chicken or house mouse IFNγ or TNFα were incubated
645 for 1 h at room temperature. The wells were then washed with PBST buffer and subsequently
646 mixed with a tetramethyl benzidine solution (ThermoFisher). The absorbance level was detected
647 at 620nm for 10 cycles of 60 s kinetic intervals with 10 s of shaking duration in a Sunrise

648 absorbance ELISA plate reader (Tecan, Männedorf, Switzerland). We then obtained the greatest
649 maximum slope of optical density/min per sample multiplied by respective serum dilution factors
650 to represent the relative levels of cytokines shown as arbitrary units.
651
652 **Determination of the titers of the antibodies against spirochetes.** The titers of IgG against
653 spirochetes were measured as described previously with modifications (94). Basically, microtiter
654 plate wells were coated with a mixture of *B. burgdorferi* B31, 297, and cN40 (1×10^6 spirochetes
655 per strain in a well). After blocking with 5% PBS-BSA, the sera from white-footed mice or robins
656 collected at 7, 14, 21, 28, and 56 days post nymph feeding were diluted in 50µl of PBS (1:100×,
657 1:300×, or 1:900×) and then added to the wells. After the samples were washed with PBST buffer,
658 the microtiter wells were incubated with antibodies that recognize the Fc region of IgG from *P.*
659 *leucopus* (1:1,000×, Serocare, Inc, Milford, MA), or wild bird (1:10,000×, Bethyl laboratory,
660 Montgomery, TX). After the addition of these antibodies, tetramethyl benzidine solution
661 (ThermoFisher) was added, and the absorbance was detected at 620nm for 10 cycles of 60 s kinetic
662 intervals with 10 s of shaking duration in a Sunrise absorbance ELISA plate reader (Tecan,
663 Männedorf, Switzerland). The values of greatest maximum slopes of optical density/min per
664 sample were multiplied by respective serum dilution factors as shown as arbitrary units,
665 representing antibody titers.
666
667 **Borreliacidal assays.** Sera collected from robins and white-footed mice at seven days post tick
668 feeding were used to measure the bactericidal activity against *B. burgdorferi* as described
669 previously (95). The complement in these serum samples was heat-inactivated by incubating these
670 samples at 55ºC for 2h. The heat inactivated sera were serially diluted in BSK-II media without

671 rabbit sera followed by being mixed with complement-preserved sera from guinea pig (Sigma-
672 Aldrich) or chicken (Biowest, Riverside). Heat-inactivated guinea pig and chicken sera were
673 included as controls. *Borrelia burgdorferi* strains B31-5A4, 297, or cN40 (1×10^7 spirochetes per
674 strain) were then mixed prior to their addition to the reaction. At 24-h after incubation, the
675 surviving spirochetes were quantified by counting the motile bacteria under dark-field microscopy
676 and presented as the proportion of serum-treated to untreated spirochetes. We also calculated the
677 50% borreliacidal titer (BA), which represents the serum dilution rate that eradicates 50% of
678 spirochetes, using dose-response stimulation fitting in GraphPad Prism 5.04.
679
680 **Statistical Analysis** Significant differences between the samples were determined using the
681 Kruskal-Wallis test followed by the two-stage step-up method of Benjamini, Krieger and Yekutieli,
682 a two tailed Fisher exact test, or a Mann−Whitney U test. A P-value less than 0.05 was considered
683 significant.
684
685 **ACKNOWLEDGEMENTS**
686 We thank Thomas Hart and Tristan Nowak for graph editing, and Jen Owen and Jean Tsao for
687 technical support in the protocol of tick infection in robins. We also thank Thomas Hart, Patricia
688 Lederman, Tristan Nowak, and Frank Blaisdell for the husbandry work to maintain tick colony
689 and robins. We are grateful for John Leong and George Chaconas for sharing the *B. burgdorferi*
690 strains B31-5A4, 297, and cN40, Sudha Chaturvedi allowing us to use her Bead Homogenizer,
691 Susan Madison-Antenucci allowing us to use her fluorescence microscope, and Noel Espina for
692 the assistance with that microscope. We thank Wadsworth Media & Tissue Culture Core for
693 preparation of *Borrelia* and American Robin and white-footed fibroblast culture medium. This

work was supported by NSF IOS-1755370 (DMT, MC and MDW), NSF-IOS1755286 (DMT, MC, MDW, YL, ADII, ALM, JS, and LDK), New York State Department of Health Wadsworth Center Start-Up Grant (ALM and YL). The funders had no role in study design, data collection and analysis, decision to publish, or preparation of the manuscript. The authors declare that the research was conducted in the absence of any commercial or financial relationships that could be construed as a potential conflict of interest.

REFERENCES

1. Poulin R. KBR, Morand S. Micromammals and Macroparasites. Tokyo: Springer; 2006. 233-56 p.

2. Futuyma DJ, Moreno, G. The evolution of ecological specialization. Ann Rev Ecol Syst 1988;19:207-33.

3. Tufts DM, Hart TM, Chen GF, Kolokotronis SO, Diuk-Wasser MA, Lin YP. Outer surface protein polymorphisms linked to host-spirochete association in Lyme borreliae. Molecular microbiology. 2019.

4. Lin YP, Diuk-Wasser MA, Stevenson B, Kraiczy P. Complement Evasion Contributes to Lyme Borreliae-Host Associations. Trends in parasitology. 2020;36(7):634-45.

5. O'Keeffe KR, Oppler ZJ, Brisson D. Evolutionary ecology of Lyme *Borrelia*. Infection, genetics and evolution : journal of molecular epidemiology and evolutionary genetics in infectious diseases. 2020:104570.

6. Kurtenbach K, De Michelis S, Etti S, Schafer SM, Sewell HS, Brade V, et al. Host association of *Borrelia burgdorferi* sensu lato--the key role of host complement. Trends in microbiology. 2002;10(2):74-9.

7. Kurtenbach K, Peacey M, Rijpkema SG, Hoodless AN, Nuttall PA, Randolph SE. Differential transmission of the genospecies of *Borrelia burgdorferi* sensu lato by game birds and small rodents in England. Applied and environmental microbiology. 1998;64(4):1169-74.

8. Kurtenbach K, Schafer SM, Sewell HS, Peacey M, Hoodless A, Nuttall PA, et al. Differential survival of Lyme borreliosis spirochetes in ticks that feed on birds. Infection and immunity. 2002;70(10):5893-5.

9. Hanincova K, Ogden NH, Diuk-Wasser M, Pappas CJ, Iyer R, Fish D, et al. Fitness variation of *Borrelia burgdorferi* sensu stricto strains in mice. Applied and environmental microbiology. 2008;74(1):153-7.

10. Baum E, Hue F, Barbour AG. Experimental infections of the reservoir species *Peromyscus leucopus* with diverse strains of Borrelia burgdorferi, a Lyme disease agent. mBio. 2012;3(6):e00434-12.

11. Hanincova K, Kurtenbach K, Diuk-Wasser M, Brei B, Fish D. Epidemic spread of Lyme borreliosis, northeastern United States. Emerging infectious diseases. 2006;12(4):604-11.

12. Brisson D, Dykhuizen DE. *ospC* diversity in *Borrelia burgdorferi*: different hosts are different niches. Genetics. 2004;168(2):713-22.

13. Vuong HB, Canham CD, Fonseca DM, Brisson D, Morin PJ, Smouse PE, et al. Occurrence and transmission efficiencies of *Borrelia burgdorferi ospC* types in avian and mammalian wildlife. Infection, genetics and evolution : journal of molecular epidemiology and evolutionary genetics in infectious diseases. 2014;27:594-600.

14. Kurtenbach K, Hanincova K, Tsao JI, Margos G, Fish D, Ogden NH. Fundamental processes in the evolutionary ecology of Lyme borreliosis. Nature reviews Microbiology. 2006;4(9):660-9.

15. Haven J, Magori K, Park AW. Ecological and inhost factors promoting distinct parasite life-history strategies in Lyme borreliosis. Epidemics. 2012;4(3):152-7.

16. Qiu WG, Bosler EM, Campbell JR, Ugine GD, Wang IN, Luft BJ, et al. A population genetic study of *Borrelia burgdorferi* sensu stricto from eastern Long Island, New York, suggested frequency-dependent selection, gene flow and host adaptation. Hereditas. 1997;127(3):203-16.

17. Qiu WG, Dykhuizen DE, Acosta MS, Luft BJ. Geographic uniformity of the Lyme disease spirochete (*Borrelia burgdorferi*) and its shared history with tick vector (*Ixodes scapularis*) in the Northeastern United States. Genetics. 2002;160(3):833-49.

18. Brisson D, Dykhuizen DE, Ostfeld RS. Conspicuous impacts of inconspicuous hosts on the Lyme disease epidemic. Proc Biol Sci. 2008;275(1631):227-35.

19. Brisson D, Baxamusa N, Schwartz I, Wormser GP. Biodiversity of *Borrelia burgdorferi* strains in tissues of Lyme disease patients. PloS one. 2011;6(8):e22926.

20. Xu Q, Seemanapalli SV, McShan K, Liang FT. Constitutive expression of outer surface protein C diminishes the ability of *Borrelia burgdorferi* to evade specific humoral immunity. Infection and immunity. 2006;74(9):5177-84.

21. Tilly K, Krum JG, Bestor A, Jewett MW, Grimm D, Bueschel D, et al. *Borrelia burgdorferi* OspC protein required exclusively in a crucial early stage of mammalian infection. Infection and immunity. 2006;74(6):3554-64.

22. Liang FT, Yan J, Mbow ML, Sviat SL, Gilmore RD, Mamula M, et al. *Borrelia burgdorferi* changes its surface antigenic expression in response to host immune responses. Infection and immunity. 2004;72(10):5759-67.

23. Andersson M, Scherman K, Raberg L. Multiple-strain infections of *Borrelia afzelii*: a role for within-host interactions in the maintenance of antigenic diversity? Am Nat. 2013;181(4):545-54.

24. Brisson D, Dykhuizen DE. A modest model explains the distribution and abundance of *Borrelia burgdorferi* strains. The American journal of tropical medicine and hygiene. 2006;74(4):615-22.

25. Haven J, Vargas LC, Mongodin EF, Xue V, Hernandez Y, Pagan P, et al. Pervasive recombination and sympatric genome diversification driven by frequency-dependent selection in *Borrelia burgdorferi*, the Lyme disease bacterium. Genetics. 2011;189(3):951-66.

26. Woolhouse ME, Taylor LH, Haydon DT. Population biology of multihost pathogens. Science. 2001;292(5519):1109-12.

27. Gog JR, Grenfell BT. Dynamics and selection of many-strain pathogens. Proceedings of the National Academy of Sciences of the United States of America. 2002;99(26):17209-14.

28. Barrett LG, Thrall PH, Burdon JJ, Linde CC. Life history determines genetic structure and evolutionary potential of host-parasite interactions. Trends Ecol Evol. 2008;23(12):678-85.

29. Barthold SW, Persing DH, Armstrong AL, Peeples RA. Kinetics of *Borrelia burgdorferi* dissemination and evolution of disease after intradermal inoculation of mice. The American journal of pathology. 1991;139(2):263-73.

30. Caine JA, Lin YP, Kessler JR, Sato H, Leong JM, Coburn J. *Borrelia burgdorferi* outer surface protein C (OspC) binds complement component C4b and confers bloodstream survival. Cellular microbiology. 2017.

31. Hart T, Nguyen NTT, Nowak NA, Zhang F, Linhardt RJ, Diuk-Wasser M, et al. Polymorphic factor H-binding activity of CspA protects Lyme borreliae from the host complement in feeding ticks to facilitate tick-to-host transmission. PLoS pathogens. 2018;14(5):e1007106.

32. Frye AM, Hart TM, Tufts DM, Ram S, Diuk-Wasser MA, Kraiczy P, et al. A soft tick *Ornithodoros moubata* salivary protein OmCI is a potent inhibitor to prevent avian complement activation. Ticks and tick-borne diseases. 2020;11(2):101354.

33. Finnie JA, Stewart RB, Aston WP. A comparison of cobra venom factor-induced depletion of serum C3 in eight different strains of mice. Dev Comp Immunol. 1981;5(4):697-701.

34. Ivanova L, Christova I, Neves V, Aroso M, Meirelles L, Brisson D, et al. Comprehensive seroprofiling of sixteen *B. burgdorferi* OspC: implications for Lyme disease diagnostics design. Clinical immunology. 2009;132(3):393-400.

35. States SL, Brinkerhoff RJ, Carpi G, Steeves TK, Folsom-O'Keefe C, DeVeaux M, et al. Lyme disease risk not amplified in a species-poor vertebrate community: similar *Borrelia burgdorferi* tick infection prevalence and OspC genotype frequencies. Infection, genetics and evolution : journal of molecular epidemiology and evolutionary genetics in infectious diseases. 2014;27:566-75.

36. Wormser GP, Brisson D, Liveris D, Hanincova K, Sandigursky S, Nowakowski J, et al. *Borrelia burgdorferi* genotype predicts the capacity for hematogenous dissemination during early Lyme disease. The Journal of infectious diseases. 2008;198(9):1358-64.

37. Jones KL, Glickstein LJ, Damle N, Sikand VK, McHugh G, Steere AC. *Borrelia burgdorferi* genetic markers and disseminated disease in patients with early Lyme disease. Journal of clinical microbiology. 2006;44(12):4407-13.

38. Wang G, Ojaimi C, Wu H, Saksenberg V, Iyer R, Liveris D, et al. Disease severity in a murine model of lyme borreliosis is associated with the genotype of the infecting *Borrelia burgdorferi* sensu stricto strain. The Journal of infectious diseases. 2002;186(6):782-91.

39. Parveen N, Robbins D, Leong JM. Strain variation in glycosaminoglycan recognition influences cell-type-specific binding by lyme disease spirochetes. Infection and immunity. 1999;67(4):1743-9.

40. Zipfel PF, Skerka C. Complement regulators and inhibitory proteins. Nature reviews Immunology. 2009;9(10):729-40.

41. Sjoberg AP, Trouw LA, Blom AM. Complement activation and inhibition: a delicate balance. Trends in immunology. 2009;30(2):83-90.

42. Tracy KE, Baumgarth N. *Borrelia burgdorferi* Manipulates Innate and Adaptive Immunity to Establish Persistence in Rodent Reservoir Hosts. Frontiers in immunology. 2017;8:116.

43. Hyde JA. Borrelia burgdorferi Keeps Moving and Carries on: A Review of Borrelial Dissemination and Invasion. Frontiers in immunology. 2017;8:114.

44. Liu N, Montgomery RR, Barthold SW, Bockenstedt LK. Myeloid differentiation antigen 88 deficiency impairs pathogen clearance but does not alter inflammation in *Borrelia burgdorferi*-infected mice. Infection and immunity. 2004;72(6):3195-203.

45. Bolz DD, Sundsbak RS, Ma Y, Akira S, Kirschning CJ, Zachary JF, et al. MyD88 plays a unique role in host defense but not arthritis development in Lyme disease. Journal of immunology. 2004;173(3):2003-10.

46. Troy EB, Lin T, Gao L, Lazinski DW, Camilli A, Norris SJ, et al. Understanding barriers to *Borrelia burgdorferi* dissemination during infection using massively parallel sequencing. Infection and immunity. 2013;81(7):2347-57.

47. Strle K, Jones KL, Drouin EE, Li X, Steere AC. *Borrelia burgdorferi* RST1 (OspC type A) genotype is associated with greater inflammation and more severe Lyme disease. The American journal of pathology. 2011;178(6):2726-39.

48. Cerar T, Strle F, Stupica D, Ruzic-Sabljic E, McHugh G, Steere AC, et al. Differences in Genotype, Clinical Features, and Inflammatory Potential of *Borrelia burgdorferi* sensu stricto Strains from Europe and the United States. Emerging infectious diseases. 2016;22(5):818-27.

49. Petzke MM, Iyer R, Love AC, Spieler Z, Brooks A, Schwartz I. *Borrelia burgdorferi* induces a type I interferon response during early stages of disseminated infection in mice. BMC microbiology. 2016;16:29.

50. Mason LM, Herkes EA, Krupna-Gaylord MA, Oei A, van der Poll T, Wormser GP, et al. *Borrelia burgdorferi* clinical isolates induce human innate immune responses that are not dependent on genotype. Immunobiology. 2015;220(10):1141-50.

51. Wang G, Petzke MM, Iyer R, Wu H, Schwartz I. Pattern of proinflammatory cytokine induction in RAW264.7 mouse macrophages is identical for virulent and attenuated *Borrelia burgdorferi*. Journal of immunology. 2008;180(12):8306-15.

52. Kern A, Schnell G, Bernard Q, Boeuf A, Jaulhac B, Collin E, et al. Heterogeneity of *Borrelia burgdorferi* Sensu Stricto Population and Its Involvement in *Borrelia* Pathogenicity: Study on Murine Model with Specific Emphasis on the Skin Interface. PloS one. 2015;10(7):e0133195.

53. Schramm F, Kern A, Barthel C, Nadaud S, Meyer N, Jaulhac B, et al. Microarray analyses of inflammation response of human dermal fibroblasts to different strains of *Borrelia burgdorferi* sensu stricto. PloS one. 2012;7(6):e40046.

54. Li X, McHugh GA, Damle N, Sikand VK, Glickstein L, Steere AC. Burden and viability of *Borrelia burgdorferi* in skin and joints of patients with erythema migrans or lyme arthritis. Arthritis and rheumatism. 2011;63(8):2238-47.

55. Jones KL, McHugh GA, Glickstein LJ, Steere AC. Analysis of *Borrelia burgdorferi* genotypes in patients with Lyme arthritis: High frequency of ribosomal RNA intergenic spacer type 1 strains in antibiotic-refractory arthritis. Arthritis and rheumatism. 2009;60(7):2174-82.

56. Dykhuizen DE, Brisson D, Sandigursky S, Wormser GP, Nowakowski J, Nadelman RB, et al. The propensity of different *Borrelia burgdorferi* sensu stricto genotypes to cause disseminated infections in humans. The American journal of tropical medicine and hygiene. 2008;78(5):806-10.

57. Barthold SW, Bockenstedt LK. Passive immunizing activity of sera from mice infected with *Borrelia burgdorferi*. Infection and immunity. 1993;61(11):4696-702.

58. Fikrig E, Bockenstedt LK, Barthold SW, Chen M, Tao H, Ali-Salaam P, et al. Sera from patients with chronic Lyme disease protect mice from Lyme borreliosis. The Journal of infectious diseases. 1994;169(3):568-74.

59. Wang G, Ojaimi C, Iyer R, Saksenberg V, McClain SA, Wormser GP, et al. Impact of genotypic variation of *Borrelia burgdorferi* sensu stricto on kinetics of dissemination and severity of disease in C3H/HeJ mice. Infection and immunity. 2001;69(7):4303-12.

60. Benoit VM, Fischer JR, Lin YP, Parveen N, Leong JM. Allelic variation of the Lyme disease spirochete adhesin DbpA influences spirochetal binding to decorin, dermatan sulfate, and mammalian cells. Infection and immunity. 2011;79(9):3501-9.

61. Roberts WC, Mullikin BA, Lathigra R, Hanson MS. Molecular analysis of sequence heterogeneity among genes encoding decorin binding proteins A and B of *Borrelia burgdorferi* sensu lato. Infection and immunity. 1998;66(11):5275-85.

62. Wilske B, Preac-Mursic V, Jauris S, Hofmann A, Pradel I, Soutschek E, et al. Immunological and molecular polymorphisms of OspC, an immunodominant major outer surface protein of *Borrelia burgdorferi*. Infection and immunity. 1993;61(5):2182-91.

63. Lin YP, Tan X, Caine JA, Castellanos M, Chaconas G, Coburn J, et al. Strain-specific joint invasion and colonization by Lyme disease spirochetes is promoted by outer surface protein C. PLoS pathogens. 2020;16(5):e1008516.

64. Lin YP, Benoit V, Yang X, Martinez-Herranz R, Pal U, Leong JM. Strain-specific variation of the decorin-binding adhesin DbpA influences the tissue tropism of the lyme disease spirochete. PLoS pathogens. 2014;10(7):e1004238.

65. Isogai E, Tanaka S, Braga IS, 3rd, Itakura C, Isogai H, Kimura K, et al. Experimental *Borrelia garinii* infection of Japanese quail. Infection and immunity. 1994;62(8):3580-2.

66. Schwan TG, Piesman J, Golde WT, Dolan MC, Rosa PA. Induction of an outer surface protein on *Borrelia burgdorferi* during tick feeding. Proceedings of the National Academy of Sciences of the United States of America. 1995;92(7):2909-13.

67. Hodzic E, Feng S, Freet KJ, Borjesson DL, Barthold SW. *Borrelia burgdorferi* population kinetics and selected gene expression at the host-vector interface. Infection and immunity. 2002;70(7):3382-8.

68. Hodzic E, Feng S, Freet KJ, Barthold SW. *Borrelia burgdorferi* population dynamics and prototype gene expression during infection of immunocompetent and immunodeficient mice. Infection and immunity. 2003;71(9):5042-55.

69. Bykowski T, Woodman ME, Cooley AE, Brissette CA, Brade V, Wallich R, et al. Coordinated expression of *Borrelia burgdorferi* complement regulator-acquiring surface proteins during the Lyme disease spirochete's mammal-tick infection cycle. Infection and immunity. 2007;75(9):4227-36.

70. Iyer R, Caimano MJ, Luthra A, Axline D, Jr., Corona A, Iacobas DA, et al. Stage-specific global alterations in the transcriptomes of Lyme disease spirochetes during tick feeding and following mammalian host adaptation. Molecular microbiology. 2015;95(3):509-38.

71. Zhang JR, Hardham JM, Barbour AG, Norris SJ. Antigenic variation in Lyme disease borreliae by promiscuous recombination of VMP-like sequence cassettes. Cell. 1997;89(2):275-85.

72. Verhey TB, Castellanos M, Chaconas G. Analysis of recombinational switching at the antigenic variation locus of the Lyme spirochete using a novel PacBio sequencing pipeline. Molecular microbiology. 2018;107(1):104-15.

73. Coutte L, Botkin DJ, Gao L, Norris SJ. Detailed analysis of sequence changes occurring during *vlsE* antigenic variation in the mouse model of *Borrelia burgdorferi* infection. PLoS pathogens. 2009;5(2):e1000293.

74. Shih CM, Telford SR, 3rd, Pollack RJ, Spielman A. Rapid dissemination by the agent of Lyme disease in hosts that permit fulminating infection. Infection and immunity. 1993;61(6):2396-9.

75. Lagal V, Portnoi D, Faure G, Postic D, Baranton G. *Borrelia burgdorferi* sensu stricto invasiveness is correlated with OspC-plasminogen affinity. Microbes and infection / Institut Pasteur. 2006;8(3):645-52.

76. Rogers EA, Marconi RT. Delineation of species-specific binding properties of the CspZ protein (BBH06) of Lyme disease spirochetes: evidence for new contributions to the pathogenesis of Borrelia spp. Infection and immunity. 2007;75(11):5272-81.

77. Wallich R, Pattathu J, Kitiratschky V, Brenner C, Zipfel PF, Brade V, et al. Identification and functional characterization of complement regulator-acquiring surface protein 1 of the Lyme disease spirochetes *Borrelia afzelii* and *Borrelia garinii*. Infection and immunity. 2005;73(4):2351-9.

78. Hammerschmidt C, Koenigs A, Siegel C, Hallstrom T, Skerka C, Wallich R, et al. Versatile roles of CspA orthologs in complement inactivation of serum-resistant Lyme disease spirochetes. Infection and immunity. 2014;82(1):380-92.

79. Alitalo A, Meri T, Comstedt P, Jeffery L, Tornberg J, Strandin T, et al. Expression of complement factor H binding immunoevasion proteins in *Borrelia garinii* isolated from patients with neuroborreliosis. European journal of immunology. 2005;35(10):3043-53.

80. Xie J, Zhi H, Garrigues RJ, Keightley A, Garcia BL, Skare JT. Structural determination of the complement inhibitory domain of *Borrelia burgdorferi* BBK32 provides insight into classical pathway complement evasion by Lyme disease spirochetes. PLoS pathogens. 2019;15(3):e1007659.

81. Margos G, Vollmer SA, Cornet M, Garnier M, Fingerle V, Wilske B, et al. A new *Borrelia* species defined by multilocus sequence analysis of housekeeping genes. Applied and environmental microbiology. 2009;75(16):5410-6.

82. Norte AC, Margos G, Becker NS, Albino Ramos J, Nuncio MS, Fingerle V, et al. Host dispersal shapes the population structure of a tick-borne bacterial pathogen. Mol Ecol. 2019.

83. Barbour AG. Isolation and cultivation of Lyme disease spirochetes. The Yale journal of biology and medicine. 1984;57(4):521-5.

84. Marcinkiewicz AL, Dupuis AP, 2nd, Zamba-Campero M, Nowak N, Kraiczy P, Ram S, et al. Blood treatment of Lyme borreliae demonstrates the mechanism of CspZ-mediated complement evasion to promote systemic infection in vertebrate hosts. Cellular microbiology. 2019;21(2):e12998.

85. Purser JE, Norris SJ. Correlation between plasmid content and infectivity in *Borrelia burgdorferi*. Proceedings of the National Academy of Sciences of the United States of America. 2000;97(25):13865-70.

86. Blevins JS, Hagman KE, Norgard MV. Assessment of decorin-binding protein A to the infectivity of *Borrelia burgdorferi* in the murine models of needle and tick infection. BMC microbiology. 2008;8:82.

87. Chan K, Casjens S, Parveen N. Detection of established virulence genes and plasmids to differentiate *Borrelia burgdorferi* strains. Infection and immunity. 2012;80(4):1519-29.

88. Marcinkiewicz AL, Lieknina I, Yang X, Lederman PL, Hart TM, Yates J, et al. The Factor H-Binding Site of CspZ as a Protective Target against Multistrain, Tick-Transmitted Lyme Disease. Infection and immunity. 2020;88(5).

89. Izuogu AO, McNally KL, Harris SE, Youseff BH, Presloid JB, Burlak C, et al. Interferon signaling in *Peromyscus leucopus* confers a potent and specific restriction to vector-borne flaviviruses. PloS one. 2017;12(6):e0179781.

90. Calhoon EA, Miller, M. K., Jimenez, A. G., Harper, J. M., Williams, J. B. Changes in cultured dermal fibroblasts during early passages across five wild bird species. Canadian Journal of Zoology. 2013;91:653-9.

91. Kern A, Zhou CW, Jia F, Xu Q, Hu LT. Live-vaccinia virus encapsulation in pH-sensitive polymer increases safety of a reservoir-targeted Lyme disease vaccine by targeting gastrointestinal release. Vaccine. 2016;34(38):4507-13.

92. Johnston E, Tsao JI, Munoz JD, Owen J. *Anaplasma phagocytophilum* infection in American robins and gray catbirds: an assessment of reservoir competence and disease in captive wildlife. Journal of medical entomology. 2013;50(1):163-70.

93. Varkey R, Du Q, Karnell JL, Xiao X, Casey KA, Woods R, et al. Discovery and characterization of potent IL-21 neutralizing antibodies via a novel alternating antigen immunization and humanization strategy. PloS one. 2019;14(1):e0211236.

94. Lin YP, Yu Y, Marcinkiewicz AL, Lederman P, Hart TM, Zhang F, et al. Non-anticoagulant Heparin as a Pre-exposure Prophylaxis Prevents Lyme Disease Infection. ACS Infect Dis. 2020;6(3):503-14.

95. Marcinkiewicz AL, Lieknina I, Kotelovica S, Yang X, Kraiczy P, Pal U, et al. Eliminating Factor H-Binding Activity of *Borrelia burgdorferi* CspZ Combined with Virus-Like Particle Conjugation Enhances Its Efficacy as a Lyme Disease Vaccine. Frontiers in immunology. 2018;9:181.

96. Burgdorfer W, Barbour AG, Hayes SF, Benach JL, Grunwaldt E, Davis JP. Lyme disease-a tick-borne spirochetosis? Science. 1982;216(4552):1317-9.

97. Leong JM, Moitoso de Vargas L, Isberg RR. Binding of cultured mammalian cells to immobilized bacteria. Infection and immunity. 1992;60(2):683-6.

98. Steere AC, Grodzicki RL, Kornblatt AN, Craft JE, Barbour AG, Burgdorfer W, et al. The spirochetal etiology of Lyme disease. The New England journal of medicine. 1983;308(13):733-40.

99. Barthold SW, de Souza MS, Janotka JL, Smith AL, Persing DH. Chronic Lyme borreliosis in the laboratory mouse. The American journal of pathology. 1993;143(3):959-71.

100. Barthold SW, Beck DS, Hansen GM, Terwilliger GA, Moody KD. Lyme borreliosis in selected strains and ages of laboratory mice. The Journal of infectious diseases. 1990;162(1):133-8.

101. Sadziene A, Wilske B, Ferdows MS, Barbour AG. The cryptic *ospC* gene of *Borrelia burgdorferi* B31 is located on a circular plasmid. Infection and immunity. 1993;61(5):2192-5.

102. Lin T, Oliver JH, Jr., Gao L. Genetic diversity of the outer surface protein C gene of southern *Borrelia* isolates and its possible epidemiological, clinical, and pathogenetic implications. Journal of clinical microbiology. 2002;40(7):2572-83.

103. Wang IN, Dykhuizen DE, Qiu W, Dunn JJ, Bosler EM, Luft BJ. Genetic diversity of *ospC* in a local population of *Borrelia burgdorferi* sensu stricto. Genetics. 1999;151(1):15-30.

104. Chan K, Awan M, Barthold SW, Parveen N. Comparative molecular analyses of *Borrelia burgdorferi* sensu stricto strains B31 and N40D10/E9 and determination of their pathogenicity. BMC microbiology. 2012;12:157.

105. Barbour AG, Travinsky B. Evolution and distribution of the *ospC* Gene, a transferable serotype determinant of *Borrelia burgdorferi*. mBio. 2010;1(4).

1006 **TABLES**

1007 **Table 1. The number of positive xenodiagnostic larval ticks collected from robins and white-**

1008 **footed mice.**

dpf[a]	Positive xenodiagnostic larval ticks acquired from			
	Mice fed on by naïve nymphs	Mice fed on by nymphs carrying *B. burgdorferi*		
		B31-5A4	297	cN40
American robins				
14	0/44	39/44[b]	19/44[b,c]	41/55[b]
28	0/44	18/33[b,c]	11/44[b,c]	46/55[b]
35	0/44	11/33[b,c]	12/44[b,c]	34/55[b]
56	0/44	8/33[b,c]	7/44[b,c]	30/55[b]
White-footed mice				
14	0/55	47/55[b,c]	47/55[b,c]	16/55[b]
28	0/33	50/55[b,c]	40/55[b,c]	8/55[b]
35	0/33	51/55[b,c]	40/55[b,c]	9/55[b]
56	0/33	38/55[b,c]	35/55[b,c]	5/55[b]

1009 [a]Days post nymph feeding.
1010 [b]Difference compared with larvae from the mice fed on by naïve nymphs by two-tailed Fisher test.
1011 [c]Difference compared with larvae from the mice fed on by nymphs carrying strain cN40 by two-
1012 tailed Fisher test.
1013

1014

1015

1016

1017

1018

1019

1020

1021

1022

1023

1024

1025 **FIGURE LEGENDS**

1026 **Figure 1. *B. burgdorferi* B31-5A4, 297, and cN40 differed in early colonization in robins and**
1027 **white-footed mice and adhesion and cytokine triggering in these animals-derived fibroblasts.**
1028 **(A and B): (A)** American robins and **(B)** white-footed (WF) mice were intradermally inoculated
1029 with 10^4 *B. burgdorferi* B31-5A4, 297, or cN40, or with BSK-II medium without rabbit sera as
1030 mock infection ("Mock"). The inoculation site of skin from these robins and mice were collected
1031 at 1-day post infection (1dpi) to determine bacterial burdens by qPCR. The bacterial loads in the
1032 tissues or blood from robins or mice were normalized to 100 ng total DNA. Shown are the
1033 geometric mean ± geometric standard deviation of bacterial burdens in those tissues from four
1034 robins or mice per group. Significant differences ($P < 0.05$ by Kruskal-Wallis test followed by the
1035 two-stage step-up method of Benjamini, Krieger and Yekutieli) in the spirochete burdens relative
1036 to the mock infected group are indicated (''*''). **(C and D):** *B. burgdorferi* B31-5A4, 297, cN40,
1037 or B314 (negative control) (2×10^6 spirochetes) were incubated with fibroblasts (2×10^5 cells) from
1038 **(C)** American robins and **(D)** white-footed (WF) mice for 1 h. We mixed those cells with FITC-
1039 conjugated goat anti-*B. burgdorferi* polyclonal antibodies and visualized the spirochetes after
1040 fixation. Additionally, DAPI was incubated with these cells to localize the nuclei from fibroblasts.
1041 The levels of spirochete attachment were evaluated by counting the number of bacteria per 50 cells
1042 under fluorescence microscopy described in the section "Materials and Methods." Each bar
1043 represents the mean of four independent determinations ± standard deviation. Asterisks indicate
1044 the significant difference ($P < 0.05$) in spirochetal attachment relative to the strain B314
1045 determined by Kruskal-Wallis test followed by the two-stage step-up method of Benjamini,
1046 Krieger and Yekutieli. **(E to J):** Fibroblasts (2×10^5 cells) from **(E to G)** American robins and **(H**
1047 **to J)** white-footed (WF) mice were incubated for 24h with *B. burgdorferi* B31-5A4, 297, or cN40

1048 (2×10^7 of spirochetes for spirochete to cell ration (MOI) at 1:100). Cell media-treated fibroblasts
1049 were included as control ("Mock"). After the RNA was extracted from these cells, the expression
1050 levels of the genes encoding IFN-γ, TNF, or TNFα-induced protein and the constitutively
1051 expressed gene, actin and 18rRNA, from robins and white-footed mice were determined using
1052 quantitative reverse transcription polymerase chain reaction. The expression levels of the genes
1053 encoding **(E and H)** 18srRNA, **(F and I)** IFNγ, **(G)** TNFα-induced protein, and **(J)** TNF are
1054 presented by normalizing to the expression levels of the gene encoding actin. Each bar represents
1055 the mean of three independent determinations ± SD. The asterisk ("*") indicates significant
1056 differences ($P < 0.05$; Kruskal-Wallis test followed by the two-stage step-up method of Benjamini,
1057 Krieger and Yekutieli) in the normalized expression levels of the gene encoding IFN-γ ,TNF, or
1058 and TNFα-induced protein in fibroblasts treated with indicated spirochete strains relative to those
1059 in mock-treated cells.
1060
1061 **Figure 2. *B. burgdorferi* B31-5A4, 297, and cN40 displayed strain-to-strain variation of**
1062 **xenodiagnostics acquisition from robins and white-footed mice. (A)** The experimental timeline
1063 of infection. **(B to K):** *I. scapularis* nymphs carrying *B. burgdorferi* B31-5A4, 297, or cN40, or
1064 naïve nymphs (Uninfect.) were allowed to feed to repletion on **(B to F)** 3, 4, 5, or 4 American
1065 robins, respectively, or **(G to K)** 5 white-footed (WF) mice per group of mice. Approximately 100
1066 larval ticks were placed on each robin at the time points indicated in Fig. S1 to feed till repletion.
1067 qPCR was used to determine spirochete burdens derived from 55 larvae feeding on the *B.*
1068 *burgdorferi*-infected white-footed mice or 33, 44, 55, and 44 larvae feeding on robins fed on by
1069 nymphs carrying B31-5A4, 297, or cN40, or uninfected nymphs, respectively. **(B and F)** The
1070 larvae were considered xenodiagnostic positive if their spirochete burdens were greater than the

1071 threshold, the mean plus three-fold standard deviation of spirochete burdens in the uninfected
1072 group. Shown are the means ± 95% SEM of percent positive larvae. **(C to F and H to K)** Shown
1073 are the geometric means ± 95% geometric standard deviation of bacterial burdens in larvae that
1074 are allowed to feed on robins or white-footed (WF) mice at **(C and H)** 14, **(D and I)** 28, **(E and**
1075 **J)** 35, and **(F and K)** 56 days post nymph feeding (dpf). Significant differences ($p < 0.05$, Kruskal-
1076 Wallis test followed by the two-stage step-up method of Benjamini, Krieger and Yekutieli) in the
1077 spirochete burdens relative to larvae feeding on naïve robins or white-footed mice (''*'') or
1078 between different groups ("#") are indicated.
1079
1080 **Figure 3. *B. burgdorferi* B31-5A4, 297, and cN40 differed in their ability to induce bacteremia**
1081 **and colonize tissues in robins and white-footed mice.** *I. scapularis* nymphs carrying *B.*
1082 *burgdorferi* B31-5A4, 297, or cN40, or naïve nymphs (Uninfect.) were allowed to feed to repletion
1083 on **(A to D and I to L)** 3, 4, 5, and 4 American robins, respectively, or **(E to H and M to P)** 5
1084 white-footed (WF) mice per group of mice. The bacterial loads in the blood at **(A and E)** 7, **(B**
1085 **and F)** 14, **(C and G)** 21, and **(D and H)** 28 days post nymph feeding (dpf) and in **(I)** skin, **(J)**
1086 heart, **(K)** brain, and **(L)** liver of robins and **(M)** ears, **(N)** tibiofemoral joints (Tibio.), **(O)** heart,
1087 **(P)** bladder of white-footed mice at 64 days post nymph feeding (dpf) were determined by qPCR.
1088 The bacterial loads in blood were normalized to 100 ng total DNA. Shown are the geometric mean
1089 ± geometric standard deviation of indicated number of robins or white-footed mice. Significant
1090 differences ($p < 0.05$, Kruskal-Wallis test followed by the two-stage step-up method of Benjamini,
1091 Krieger and Yekutieli) in the spirochete burdens relative to robins or white-footed mice fed on by
1092 naïve nymphs (''*'') are indicated.
1093

1094 **Figure 4. *B. burgdorferi* B31-5A4, 297, and cN40 varied in their ability to survive in robin**
1095 **but not white-footed mouse sera.** A high passage, non-infectious, serum sensitive *B. burgdorferi*
1096 strain B313 ("B313") or *B. burgdorferi* B31-5A4, 297, or cN40 was incubated for 4-h with the
1097 sera from American robins at a final concentration of 40% in the **(A)** absence or **(B)** presence of 2
1098 μM of OmCI. Each of these spirochete strains was also incubated for 4-h with the sera from white-
1099 footed (WF) mice at a final concentration of 40% in the **(C)** absence or **(D)** presence of 2 μM of
1100 CVF. The above-mentioned sera were also heat-inactivated and included as controls. The number
1101 of motile spirochetes was assessed microscopically. The percentage of survival for *B. burgdorferi*
1102 was calculated using the number of mobile spirochetes at 4-h post incubation normalized to that
1103 prior to the incubation with serum. The assays were performed at three independent occasions;
1104 within each experiment, samples were run in triplicate, and the survival percentage for each
1105 experiment was calculated by averaging the results from triplicate runs. The result shown here is
1106 the average ± standard deviation of the survival percentage from three independent experiments.
1107 (#), the significant difference ($P < 0.05$) of the percent survival of spirochetes between indicated
1108 groups was determined using Kruskal-Wallis test followed by the two-stage step-up method of
1109 Benjamini, Krieger and Yekutieli.
1110
1111 **Figure 5. *B. burgdorferi* B31-5A4, 297, and cN40 triggered different levels of pro-**
1112 **inflammatory cytokines at early stages of robin and white-footed mice infection.** *I. scapularis*
1113 nymphs infected with *B. burgdorferi* B31-5A4, 297, cN40, or naïve nymphs (Uninfect.) were
1114 allowed to feed to repletion on **(A to H)** American robins or **(I to P)** white-footed (WF) mice. The
1115 sera were obtained **(A, E, I, and M)** prior to tick feeding or at **(B, F, J, and N)** 7-, (**C, G, K, and**
1116 **O)** 14-, or **(D, H, L, and P)** 21-days post nymph feeding ("dpf"). The levels of IFNγ **(A to D and**

1117 **I to L)** and TNFα **(E to H and M to P)** were determined using quantitative ELISA as described
1118 in Section "Materials and Methods." Shown are the geometric mean ± geometric standard
1119 deviation of five white-footed mice per group or robins (3, 4, 5, and 4 for the strains B31-5A4-,
1120 297-, cN40-infected robins or uninfected robins per group, respectively). Significant differences
1121 ($p < 0.05$, Kruskal-Wallis test followed by the two-stage step-up method of Benjamini, Krieger
1122 and Yekutieli) in the cytokine levels relative to robins or white-footed mice fed on by naïve
1123 nymphs (''*'') are indicated.
1124
1125 **Figure 6. *B. burgdorferi* B31-5A4, 297, and cN40 differed in the ability to induce antibodies**
1126 **against spirochetes in robin and white-footed mice during infection.** *I. scapularis* nymphs
1127 infected with *B. burgdorferi* B31-5A4, 297, or cN40, or naïve nymphs (Uninfect.) were allowed
1128 to feed to repletion on **(A to E)** American robins or **(F to J)** white-footed (WF) mice. The sera
1129 were obtained at **(A and F)** 0-, **(B and G)** 7-, **(C and H)** 14-, **(D and I)** 21-, or **(E and J)** 28-days
1130 post nymph feeding ("dpf"). The levels of IgG against the mixture of *B. burgdorferi* strains B31-
1131 5A4, 297, and cN40 (1×10^6 spirochetes per strain in each microtiter well) were determined using
1132 quantitative ELISA as described in Section "Materials and Methods." Shown are the geometric
1133 mean ± geometric standard deviation of five white-footed mice or robins per group (3, 4, 5, and 4
1134 for the strains B31-5A4-, 297-, cN40-infected robins or uninfected robins per group, respectively).
1135 Significant differences ($p < 0.05$, Kruskal-Wallis test followed by the two-stage step-up method
1136 of Benjamini, Krieger and Yekutieli) in the antibody titers relative to robins or white-footed mice
1137 fed on by naive nymphs (''*'') are indicated. Sera from the **(K)** American robins and **(L)** white-
1138 footed (WF) mice at 7 days after fed on by *I. scapularis* nymphs carrying *B. burgdorferi* strains
1139 B31-5A4, 297, or cN40, or naïve nymphs (Uninfect.) were collected. These sera were serially

1140 diluted as indicated and mixed with **(K)** chicken or **(L)** guinea pig complement and the mixture of
1141 the strains B31-5A4, 297, and cN40 (1×10^7 spirochetes per strain in each reaction). After
1142 incubation for 24- h, surviving spirochetes were quantified from three fields of view for each
1143 sample microscopically. The experiment was performed at three independent occasions. The
1144 survival percentage was derived from the proportion of serum-treated to untreated spirochetes.
1145 Data shown are the mean ± standard error of the mean (SEM) of the survival percentage from three
1146 replicates in one representative experiment. The 50% borreliacidal dilution of each serum sample
1147 (50% BA), representing the dilution rate that effectively killed 50% of spirochetes, was obtained
1148 from curve-fitting and extrapolation of data shown in the table above respective panels. The 50%
1149 BA of some strain-sera pairs could not be determined because no robust killing was observed,
1150 resulting in curves that did not fit (N.F.).
1151
1152 **Figure 7. The schematic diagram showing the model supported by this study.** Upon *B.*
1153 *burgdorferi* transmission from ticks to hosts, multiple cellular and immunological mechanisms
1154 may play in concert to determine the fitness of spirochetes in hosts. These mechanisms include the
1155 ability of *B. burgdorferi* to attach to cells or tissues (spirochete adhesiveness) and escape from host
1156 immune clearance (early host defense), such as complement, cytokine-mediated responses, and
1157 antibodies. Both mechanisms applied on spirochetes would lead to host specialization, resulting in
1158 the association of *B. burgdorferi* with particular hosts (i.e. mammal or avian specialists).

Fig. 1

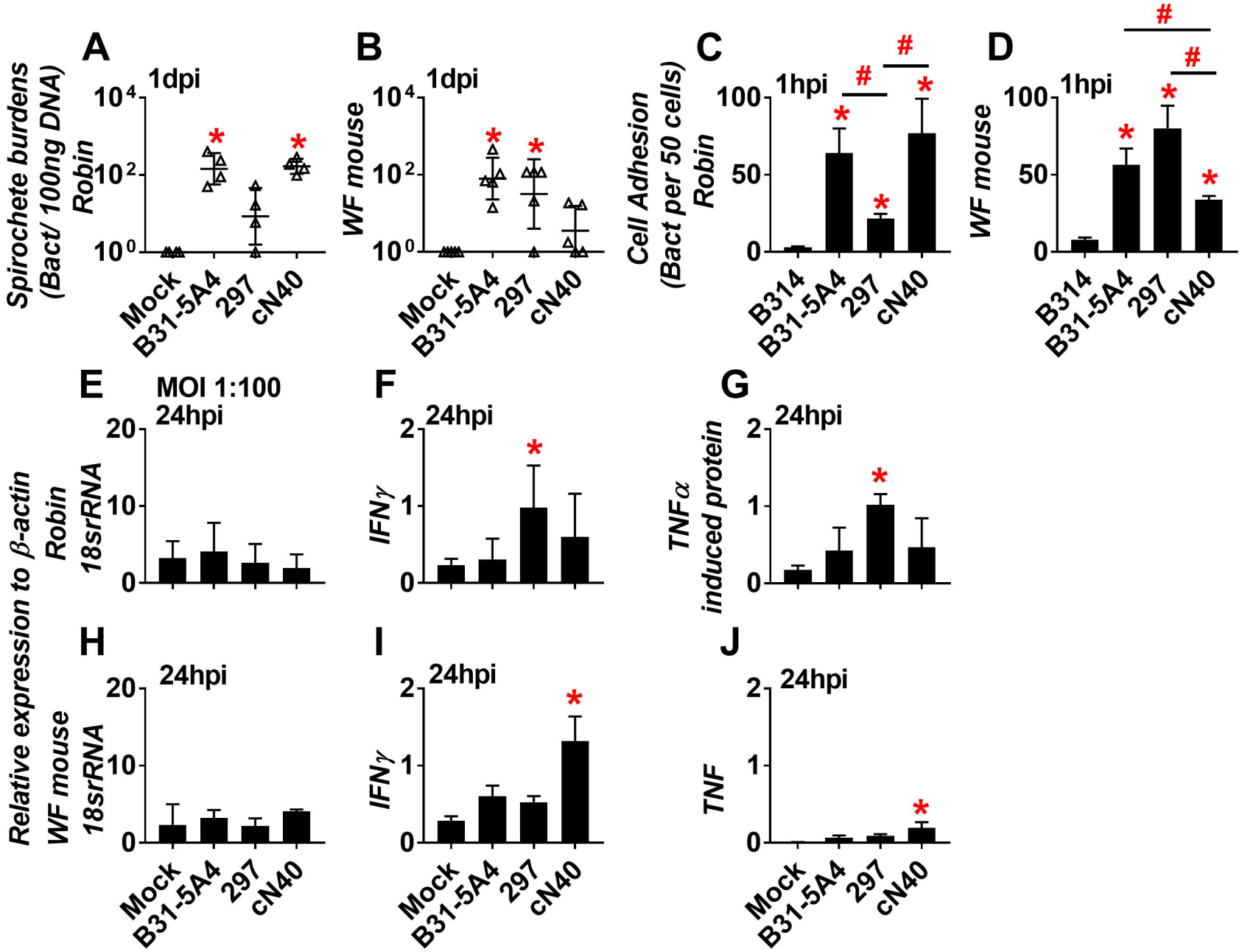
A
1dpi
Spirochete burdens (Bact/ 100ng DNA)
Robin
10^4
10^2
10^0
Mock
B31-5A4
297
cN40
B
1dpi
WF mouse
10^4
10^2
10^0
Mock
B31-5A4
297
cN40
C
1hpi
Cell Adhesion (Bact per 50 cells)
Robin
100
50
0
B314
B31-5A4
297
cN40
D
1hpi
WF mouse
100
50
0
B314
B31-5A4
297
cN40
E
MOI 1:100
24hpi
Relative expression to β-actin
Robin
18srRNA
20
10
0
F
24hpi
IFNγ
2
1
0
G
24hpi
TNFα induced protein
2
1
0
H
24hpi
WF mouse
18srRNA
20
10
0
Mock
B31-5A4
297
cN40
I
24hpi
IFNγ
2
1
0
Mock
B31-5A4
297
cN40
J
24hpi
TNF
2
1
0
Mock
B31-5A4
297
cN40

Fig. 2

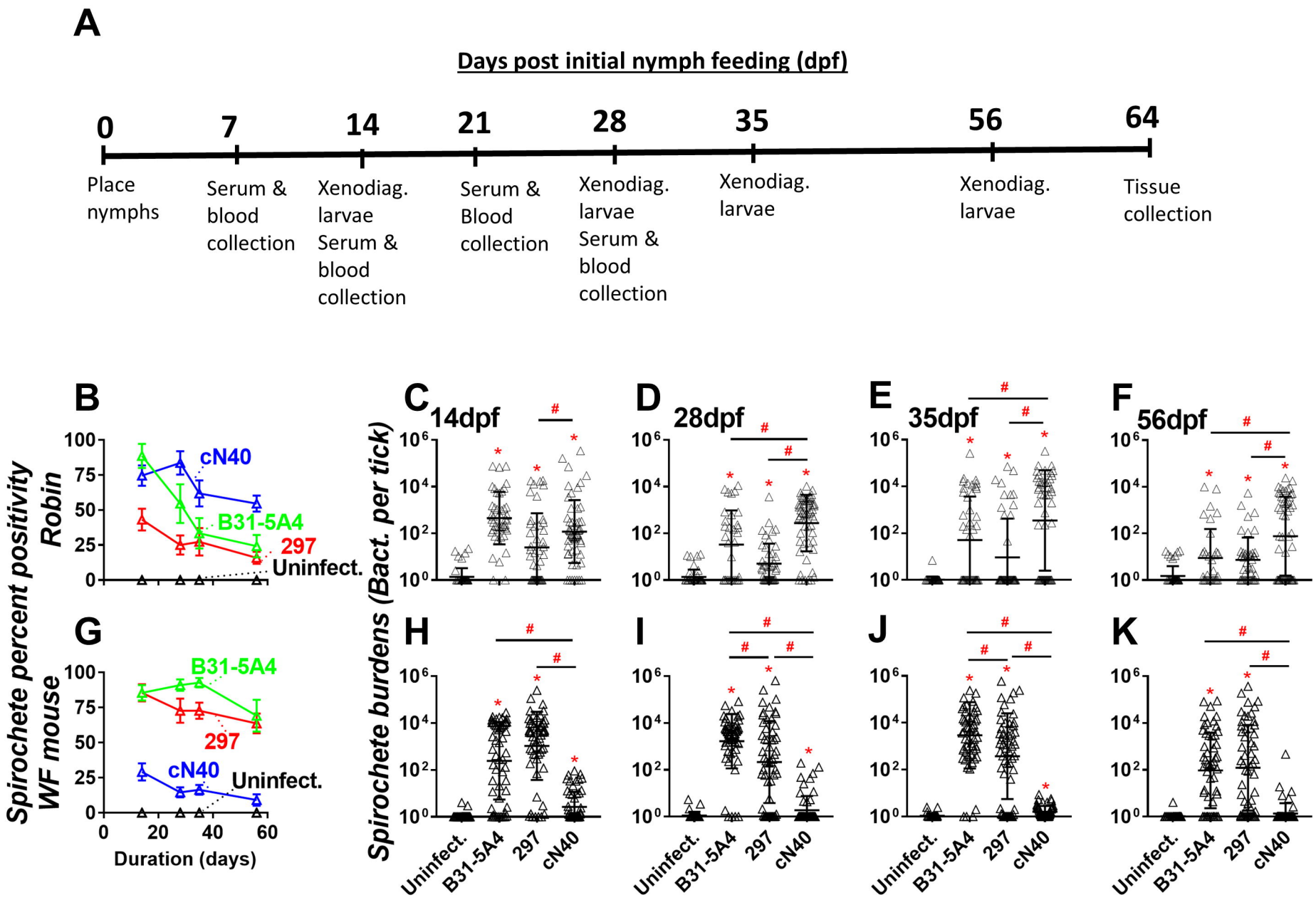
A
Days post initial nymph feeding (dpf)
0
7
14
21
28
35
56
64
Place nymphs
Serum & blood collection
Xenodiag. larvae Serum & blood collection
Serum & Blood collection
Xenodiag. larvae Serum & blood collection
Xenodiag. larvae
Xenodiag. larvae
Tissue collection
B
Spirochete percent positivity Robin
cN40
B31-5A4
297
Uninfect.
G
Spirochete percent positivity WF mouse
B31-5A4
297
cN40
Uninfect.
Duration (days)
C 14dpf
D 28dpf
E 35dpf
F 56dpf
H
I
J
K
Spirochete burdens (Bact. per tick)
Uninfect.
B31-5A4
297
cN40

Fig. 3

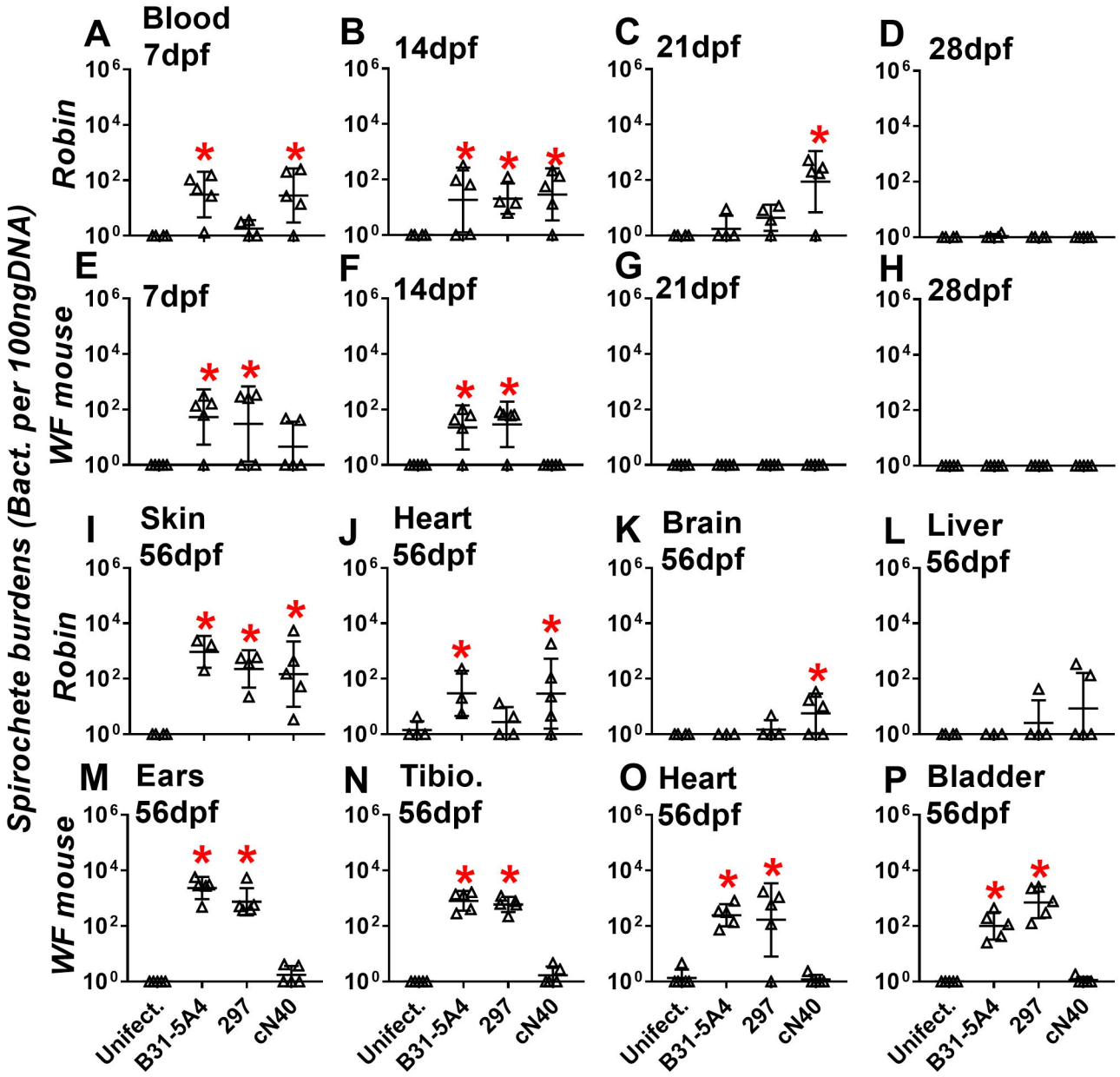
Spirochete burdens (Bact. per 100ngDNA)
A Blood 7dpf
B 14dpf
C 21dpf
D 28dpf
E 7dpf
F 14dpf
G 21dpf
H 28dpf
I Skin 56dpf
J Heart 56dpf
K Brain 56dpf
L Liver 56dpf
M Ears 56dpf
N Tibio. 56dpf
O Heart 56dpf
P Bladder 56dpf
Robin
WF mouse
10^6
10^4
10^2
10^0
Unifect.
B31-5A4
297
cN40

Fig. 4

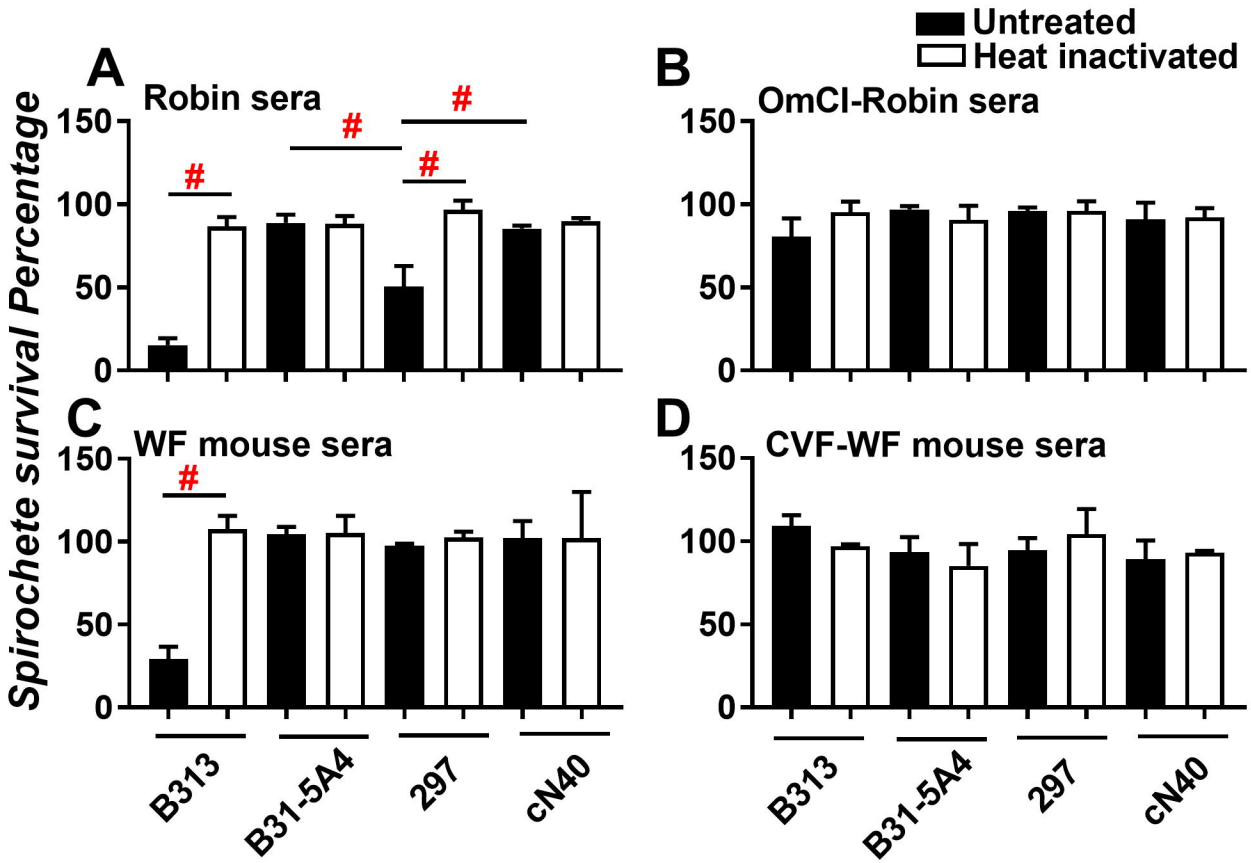
Untreated
Heat inactivated
A
Robin sera
B
OmCI-Robin sera
C
WF mouse sera
D
CVF-WF mouse sera
Spirochete survival Percentage
150
100
50
0
#
B313
B31-5A4
297
cN40

Fig. 5

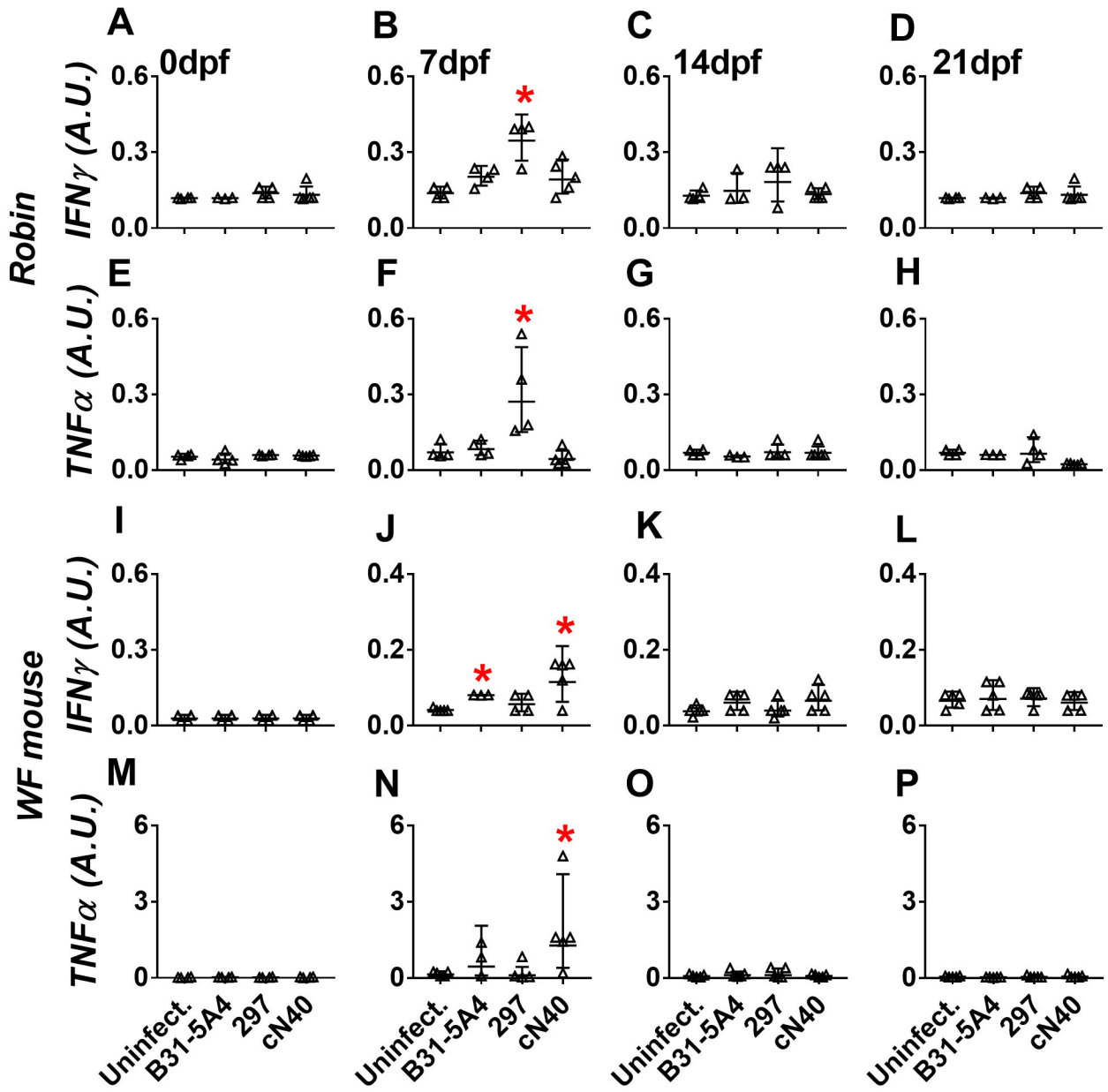
A
0dpf
B
7dpf
C
14dpf
D
21dpf
E
F
G
H
I
J
K
L
M
N
O
P
Robin
WF mouse
IFNγ (A.U.)
TNFα (A.U.)
0.6
0.3
0.0
0.4
0.2
6
3
0
*
Uninfect.
B31-5A4
297
cN40

Fig. 6

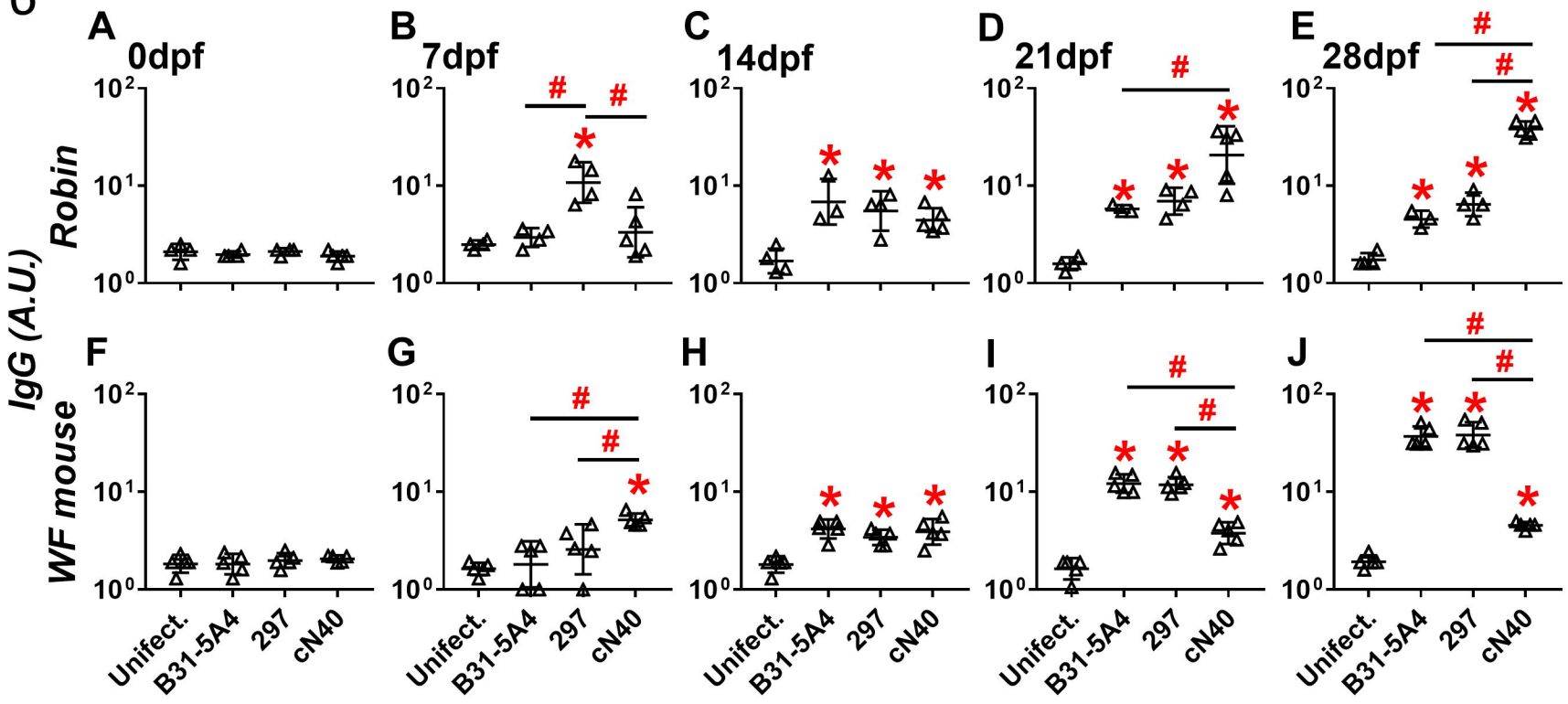

K

	Sera from Robins infected with			
	B31-5A4	297	cN40	Uninfect.
50%BA	N.F.	52±2	N.F.	N.F.

L

	Sera from WF mice infected with			
	B31-5A4	297	cN40	Uninfect.
50%BA	N.F.	N.F.	32±4	N.F.

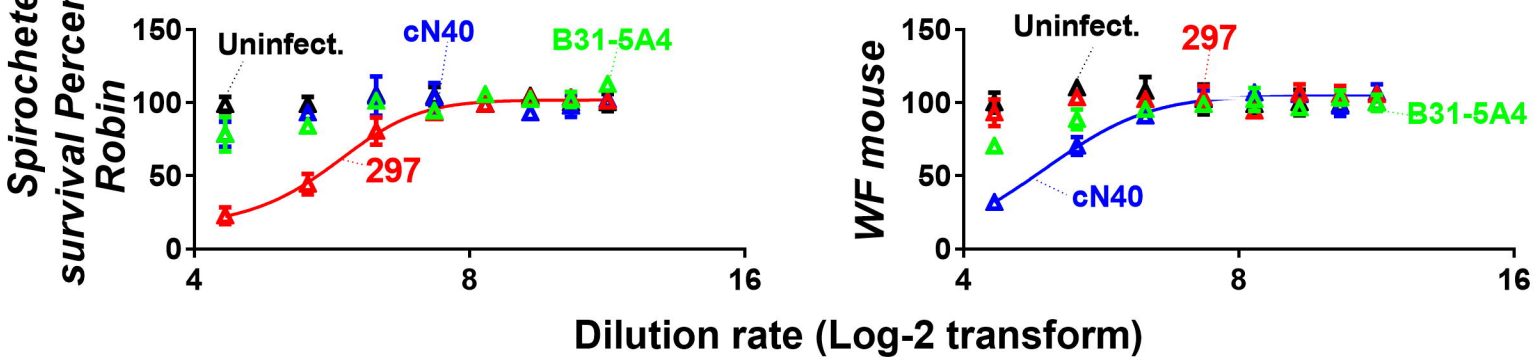

Fig. 7

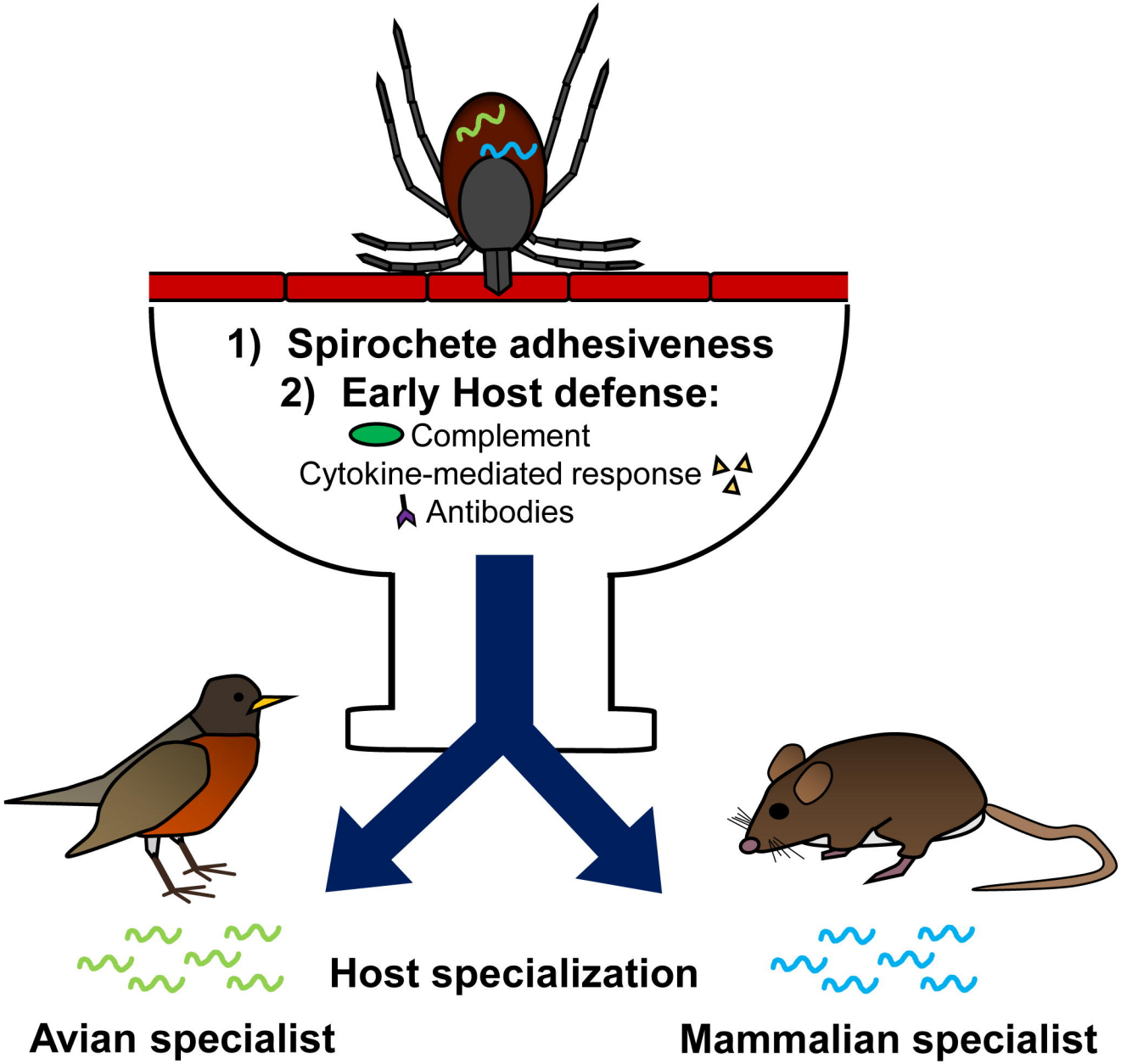
1) Spirochete adhesiveness
2) Early Host defense:
Complement
Cytokine-mediated response
Antibodies
Host specialization
Avian specialist
Mammalian specialist